REPORT DOCUMENTATION PAGE

Public reporting burden for this collection of information is estimated to average 1 hour per response, including the time for reviewing instructions, searching existing data sources, gathering and maintaining the data needed, and completing and reviewing the collection of information. Send comments regarding this burden estimate or any other aspect of this collection of information, including suggestions for reducing this burden, to Washington Headquarters Services, Directorate for Information Operations and Reports, 1215 Jefferson Davis Highway, Suite 1204, Arlington, VA 22202-4302, and to the Office of Management and Budget, Paperwork Reduction Project (0704-0188), Washington, DC 20503.

1. AGENCY USE ONLY (Leave blank)	2. REPORT DATE March 18, 1998	3. REPORT TYPE AND DATES COVERED 01 JUL 96 31 JAN 98

4. TITLE AND SUBTITLE

U.S.-Japan Research Collaboration on Hard Driving Ceramic Actuators

5. FUNDING NUMBERS

N00014-96-1-1128

6. AUTHOR(S)

Shoko Yoshikawa and Ming-Jen Pan

7. PERFORMING ORGANIZATION NAME(S) AND ADDRESS(ES)

Materials Research Laboratory
The Pennsylvania State University
University Park, PA 16802

8. PERFORMING ORGANIZATION REPORT NUMBER

9. SPONSORING / MONITORING AGENCY NAME(S) AND ADDRESS(ES)

Office of Naval Research
Ballston Center Tower One
800 North Quincy Street
Arlington, VA 22217-5660

10. SPONSORING / MONITORING AGENCY REPORT NUMBER

11. SUPPLEMENTARY NOTES

N/A

DISTRIBUTION STATEMENT A

Approved for public release;
Distribution Unlimited

12a. DISTRIBUTION / AVAILABILITY STATEMENT

Distribution unlimited

19980417 130

13. ABSTRACT (Maximum 200 words)

High field properties of electro-active ceramics are an important issue to understand in order to apply these ceramics in actuator applications. This project was developed to establish research collaborations with Japanese piezoelectric ceramic researchers in order to fully characterize these ceramics. Due to a PI change during the contract, the collaboration was not completed as originally planned. The information exchange was summarized as a trip report. However, at Penn State University, three very different family of active ceramics (electrostrictor, phase switching ceramics and various compositions of conventional PZT) were prepared and tested under high field and various pre-load and temperature conditions. The electrostrictive PMN-PT showed little stress dependence whereas the AFE-FE phase switching composition showed intriguing stress dependence which introduced a new idea of incorporating additional phase transformation steps. The tetragonal structure of conventional PZTs showed less stress dependence than the morphotropic phase boundary (MPB) and rhombohedral compositions. Stress depoling can be reduced by maintaining a DC bias. These results showed correlations between intrinsic material behavior and external stresses, both electrical and mechanical.

14. SUBJECT TERMS

Electro-active ceramics; US-Japan collaboration; Electrostrictor Phase switching ceramics; PZT; Actuator

15. NUMBER OF PAGES
56

16. PRICE CODE
N/A

17. SECURITY CLASSIFICATION OF REPORT	18. SECURITY CLASSIFICATION OF THIS PAGE	19. SECURITY CLASSIFICATION OF ABSTRACT	20. LIMITATION OF ABSTRACT
Unclassified	Unclassified	Unclassified	Unlimited

Table of Contents

1. JAPAN TRIP REPORT

During the month of August 1997, the PI traveled to Japan and visited four Japanese companies that are currently engaged in piezoelectric ceramic actuator research. The followings are the summary of these visits.

1.1 TOYOTA CENTRAL RESEARCH AND DEVELOPMENT LAB.

The research collaboration has been established with the functional ceramic group under Dr. Kamiya. Dr. Saito measured strain, polarization and acoustic emission of the samples we sent previously using their set-up. The samples were two types of active ceramics; AFE-FE phase switcher, PLSnZT, and relaxor ferroelectrics, PMN-PT. Figure 1.1.1 to 1.1.5 are some of the data provided by Dr. Saito. Due to the high switching voltage, he could not provide appropriate data for PLSnZT-A1 sample, thus no data are included. PMN-PT-La2 sample showed ferroelectric behavior at the measured temperature as shown in figure 1.1.5. The strain and polarization agreed with Penn State's measurements. Acoustic emission counts were also consistent with some of the data measured by Mr. Aburatani at Penn State on similar samples, though many technical questions remained.

In addition we have discussed piezoelectric actuator properties under uniaxial stress (stress parallel to driving field) and effects of applied electric field on fracture toughness and flexural strength of PZT ceramics with Mr. Makino. The possible analysis using fractography on the specimen after such experiments has been suggested by Dr. Pohanka.

1.2 NGK INSULATORS, LTD. and NGK SPARK PLUG CO. LTD.

The PI visited both companies on the same day, since they are located side by side. They are, however, separate companies since 1939 and there is a little competition in the area of piezoelectric devices.

Dr. Soma was the host for NGK Insulators. Their research facilities and their group's ongoing research, particularly in the area of optoelectronics were impressive. Although
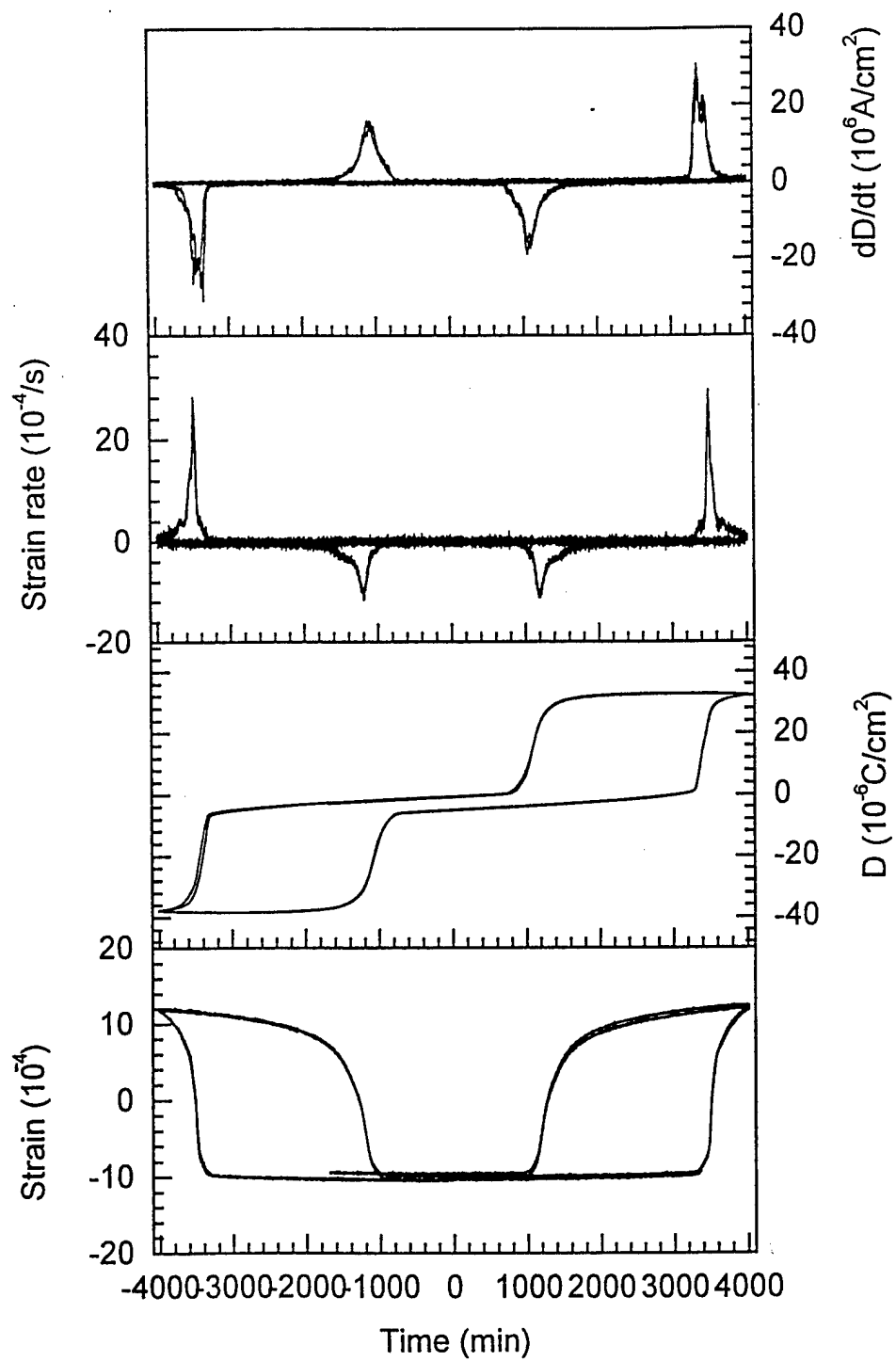
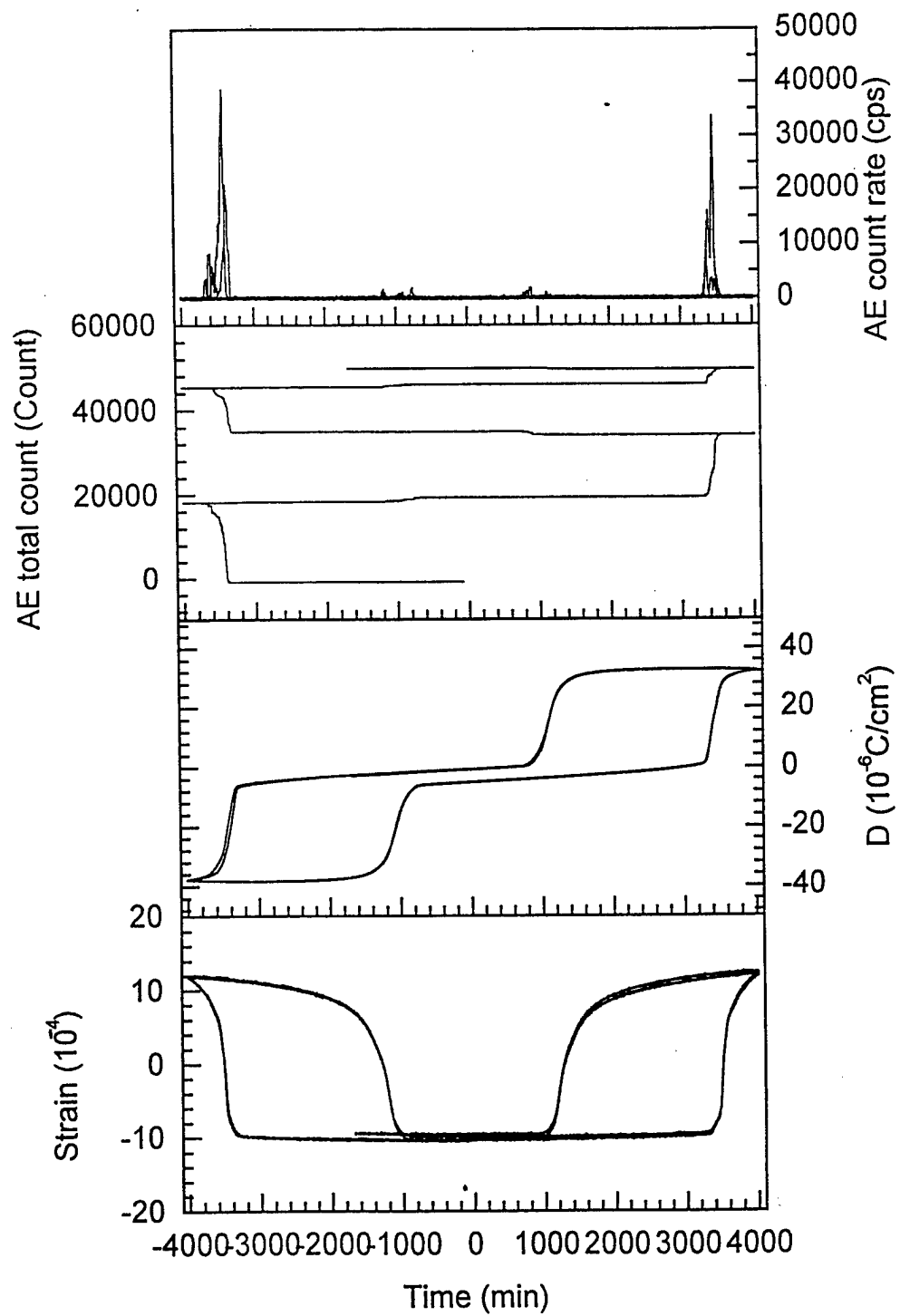Figure 1.1.1   Strain and polarization responses for PLSnZT-B

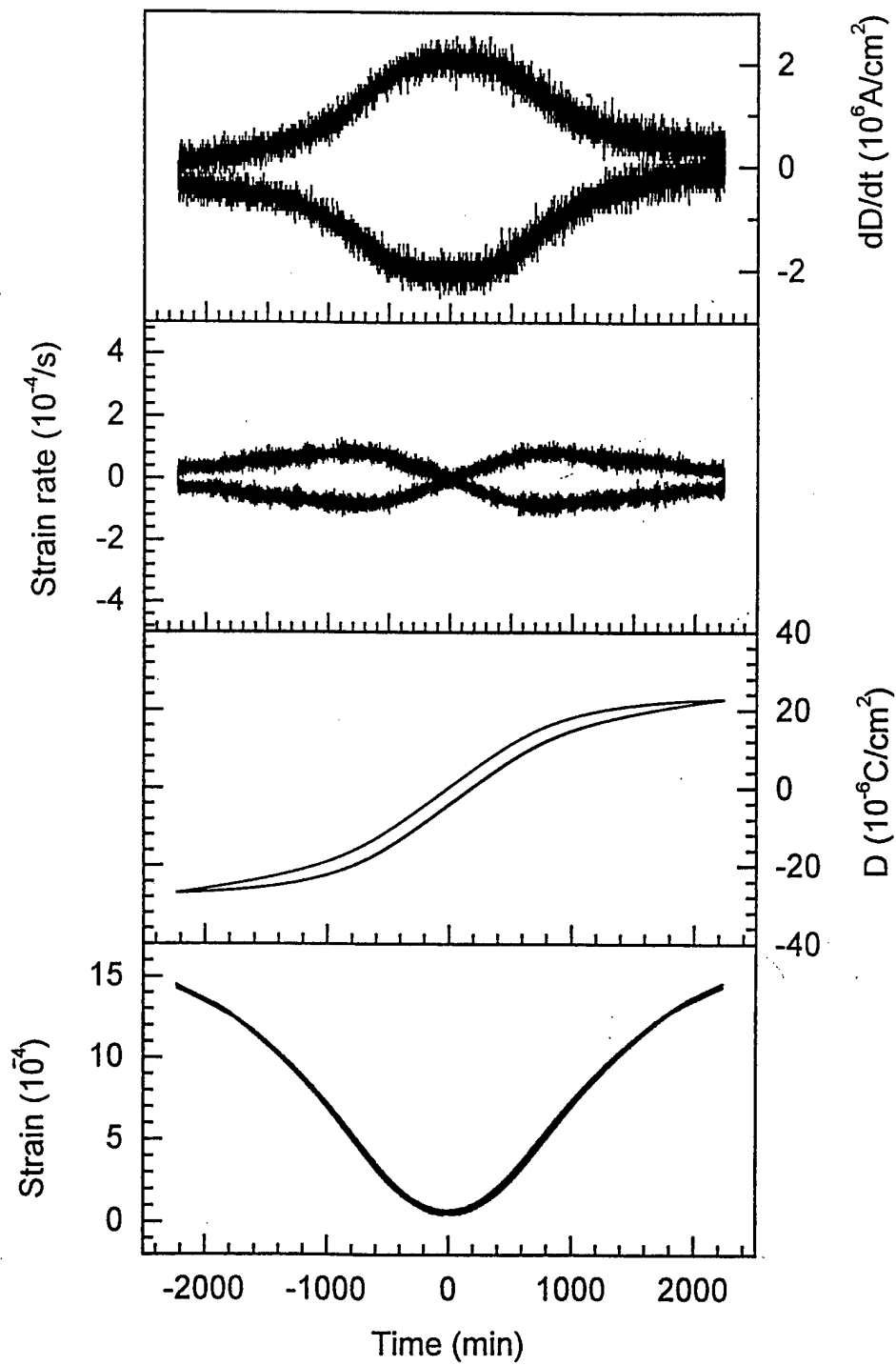Figure 1.1.2   Strain and polarization responses for PLSnZT-B

3

Figure 1.1.3   Strain and polarization responses for PMN-PT-La-1
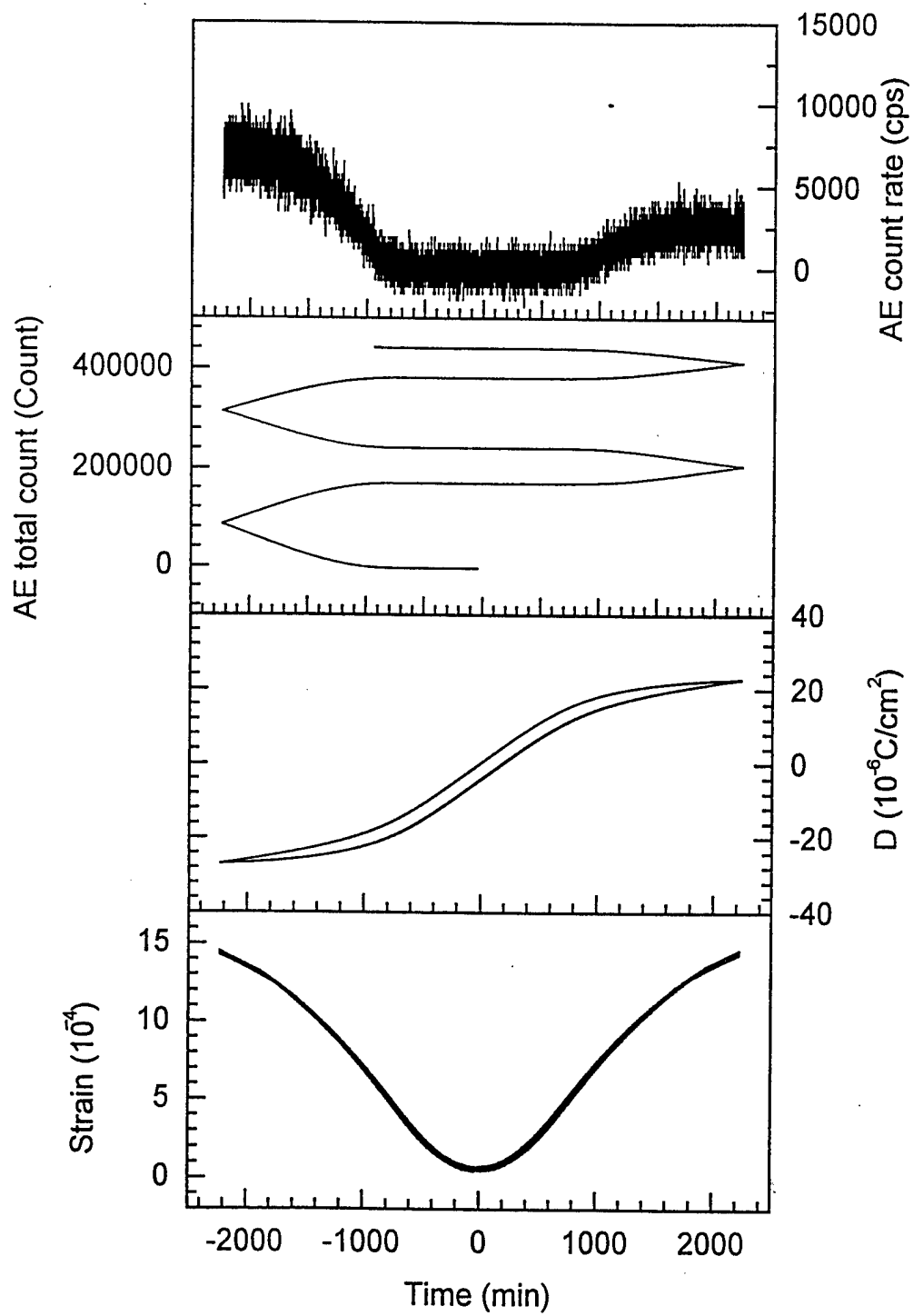
Figure 1.1.4   Strain and polarization responses for PMN-PT-La-1
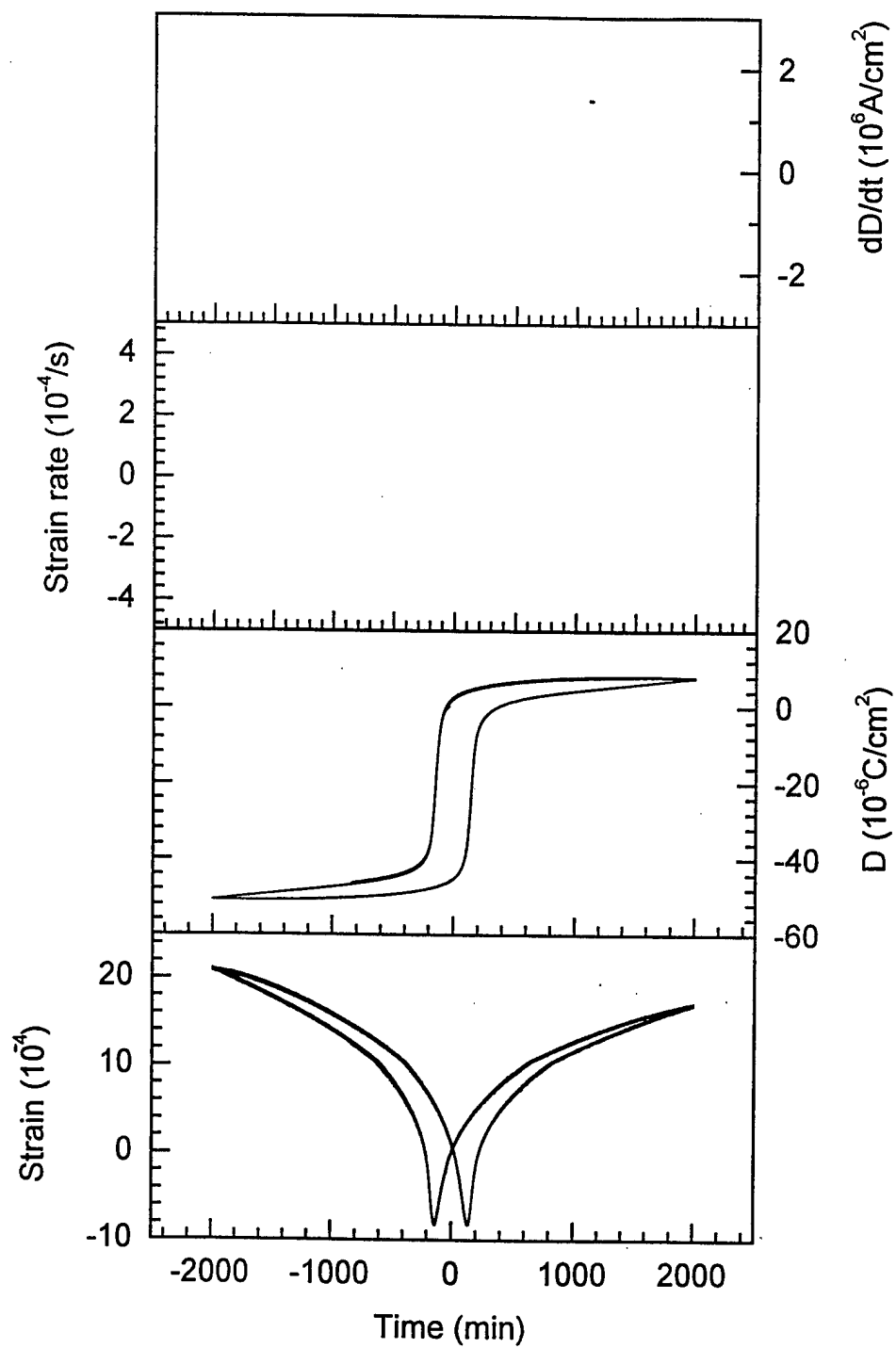
5

Figure 1.1.5   Strain and polarization responses for PMN-PT-La-2

NGK currently produces actuators for color printers, we did not discuss any research issues on PZT ceramics.

Dr. Banno was the host for NGK Spark Plugs/ NTK Technical Ceramics. The company has been well known for its development in piezoceramic/polymer composite transducers and stack actuators. The business of stack actuators, however, were not high priority in the company mostly due to their high cost and low reliability. These issues are the same in most piezoceramic actuator companies the PI has visited in both Japan and US.

1.3 TDK RESEARCH CENTER

Although the main research area at the TDK Research Center is multilayer chip capacitors, Ni electroded ones in particular, piezoelectrics have been one of the areas of their strength. Mr. Miyabe, the group leader of piezoceramic research, indicated that they are looking for new applications. The possibility of non-lead piezoelectric ceramics, development of large strain, wide temperature stable material were discussed with researchers at Narita research lab.

1.4 SUMITOMO METAL IND.

Sumitomo Metal has been producing a wide variety of piezoelectric ceramics for sensors/actuators and resonators. They produce a series of PZTs that are also HIPped (Hot Isostaically Pressed) that the PI was interested in for property comparisons. The issues with them, however, are also cost and reliability for actuator applications. There is a strong need for research for high field, high strain application yet it is difficult to justify funding due to the limitation in market size.

1.5 SUMMARY

It seems to be a trend that these well-established piezoceramic manufacturing research groups in Japan are all suffering from the slow piezoelectric actuator/sensor growth rate,

which results in difficulty to justifying research funding. In spite of the circumstance, their resources and interests are still high. The area of growth in the field is in chip resonators.

2   PENN STATE EXPERIMENTS

2.1   SAMPLE PREPARATION

Three types of electroactive ceramics were tested in this project: electrostrictors, antiferroelectrics, and conventional PZT piezoelectrics. The first two types of ceramics were provided gratis by TRS Ceramics, Inc in the form of binder-added powder. They were pressed, sintered, and assembled into actuators at Penn State for testing. PZT materials were fabricated in-house in order to control the stoichiometry. Three different compositions across the rhombohedral/tetragonal morphtropic phase boundary were chosen in order to study the trend of material response. Because the electrostrictive and antiferroelectric materials were commercially available, we followed the manufacturer's suggested processing steps. No additional compositional nor strutural analyses were performed. On the other hand, the processing of conventional PZTs was well characterized during each processing step.

Electrostrictors

Electrostrictive PMN-PT ceramics belong to a class of relaxor ferroelectrics which exhibit no macroscopic polarization. Upon the application of an electric field, a dimensional change which is proportional to the square of the field-induced polarization can be observed. Because of the low hysteresis it exhibits and consequently little heat generation and excellent position repeatability, PMN-PT is attractive for precision submicron control. The most common composition is 90% PMN-10% PT (90-10) for room temperature applications. Also, a composition with higher PT content (76-24) and thus higher field-induced ferroelectricity has been identified for use at 85°C.

Phase Switching Ceramics

The lead lanthanum stannate zirconate titanate (PLSnZT) system has been widely studied for actuator applications due to its potential of producing high strain. In this family of ceramics, the antiferroelectric tetragonal (AFE$_{tet}$) phase can be readily switched to its

9

neighboring ferroelectric rhombohedral (FE_{rh}) phase with the application of an electric field. This phase transition is accompanied by a large change in volume associated with high longitudinal strain (in the field direction). Crystallographic analyses based on X-ray diffraction have shown that 0.5% is the maximum strain possible for an ideal single crystal in this system. For polycrystalline samples, a strain of 0.2% can be readily achieved at the antiferroelectric-to-ferroelectric (AFE-FE) switching field. This study investigates the influence of pre-stress and temperature on the AFE-FE phase switching. A composition in the AFE_{tet} region, $(Pb_{0.98}La_{0.02})(Sn_{0.33}Zr_{0.55}Ti_{0.12})_{0.995}O_3$, was chosen for this study.

Conventional PZTs

PZT 56/44 (rhombohedral), PZT 52/48 (morphotropic phase boundary), PZT 48/52 (tetragonal) were investigated in this study.. All compositions were Nb-doped (2.4 atm%) in order to reduce the conductivity. PZT52/48 ceramics with different Nb doping levels (1%, 2.4% and 5%) were also investigated. During processing, the conventional mix oxide method was used. PbO, ZrO_2, TiO_2 and Nb_2O_5 were mixed according to the required composition, and ball-milled in acetone for 48 hours. The mixed powders were calcined at 900°C for 4 hours. Special care was taken to control the lead loss during sintering.

Without excess Pb: The calcined PZT powders were ball-milled in acetone for 48 hours. Pellets were pressed and sintered at 1250°C for 1.5 hour.
With excess Pb: The calcined PZT powders were ball milled in acetone for 24 hours. The milled powders were mixed with 3% (weight percent) excess PbO and ball milled for 24 hours. Pellets were pressed and sintered at 1250°C for 1.5 hour.

The grain size of the sintered PZT ceramics is about 1- 2 μm.

Table I The weight loss and density of various sintered PZT compositions without Pb compensation.

	Weight (g) before	Weight (g) after	Weight loss(%)	Density (g/cm3)	Relative Density (%)*
PZT56/44	1.5342	1.4851	3.2	7.72	96.5
PZT52/48	1.5230	1.5024	1.4	7.87	98.4
PZT48/52	1.5358	1.4960	2.6	7.78	97.2

* Theoretical Density was assumed to be 8.00 (g/cm3).

Table II The net weight loss of Pb compensated PZT compositions after sintering.

	Weight (g) before	Weight (g) after	Weight loss (%)	Net weight loss*
PZT 56/44	1.4853	1.4186	4.49	1.49
PZT52/48	1.4882	1.4321	3.76	0.76
PZT48/52	1.5097	1.4588	3.37	0.37

* The net weight loss was calculated by Weight loss(%) - 3 (%) PbO, assuming a homogenous evaporation of PbO in the pellets.

Table III The density of Pb compensated PZT compositions after sintering.

	Density (g/cm3)	Relative D (%)*
PZT56/44	7.83	97.9
PZT52/48	7.83	97.9
PZT48/52	7.86	98.3

* Theoretical Density was assumed to be 8.00 (g/cm3)

11

Figure 2.1.1 shows the X-ray Diffraction patterns of 2.4 atm% Nb-doped PZT 56/44, PZT 52/48 and PZT 48/52 ceramics. It can be seen that samples with single perovskite phase were obtained. The splitting of the XRD peaks at 21.8° and 44.5° for PZT 48/52 indicate that the structure of the sample is tetragonal, whereas the peak splitting at 38.4° for PZT 56/44 indicates that the sample has rhombohedral structure. The XRD pattern of PZT 52/48 is typical of a mixed tetragonal-rhombohedral phase.
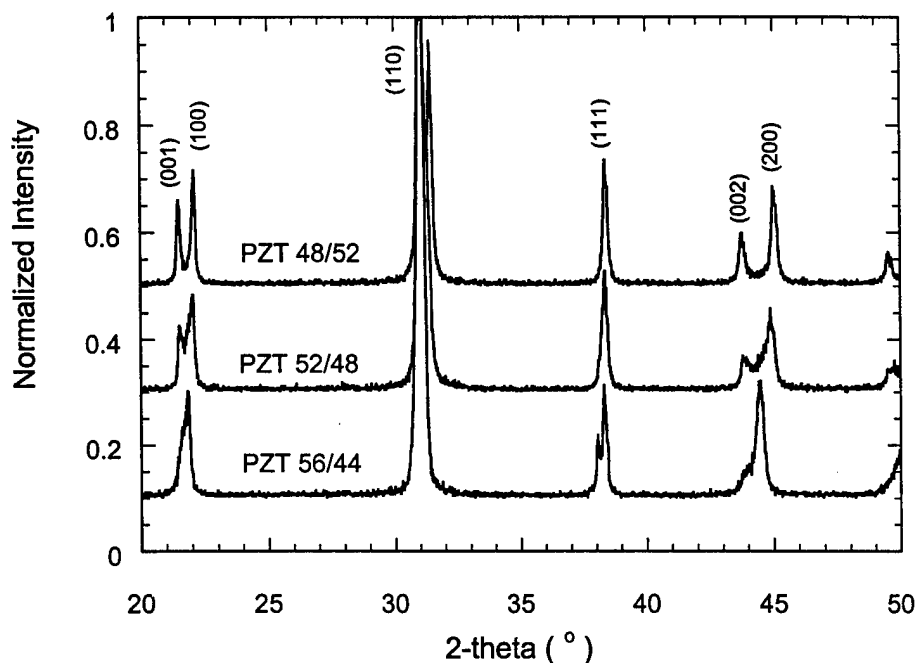
Figure 2.1.1 X-ray diffraction patterns of 2.4% Nb-doped PZT 56/44, 52/48 and 48/52 ceramics showing a tetragonal phase for PZT48/52, a rhombohedral phase for PZT 56/44 and a mixed tetragonal-rhombohedral phase for PZT52/48.

2.2   EXPERIMENTAL SETUP

An experimental setup was designed to measure the material and actuator response under both uniaxial stress and temperature (Figure 2.2.1). A rigid, precisely-guided steel frame provides true uniaxial stress during loading. The spherical washer on top of the upper contact plate further minimizes transverse force and bending moment caused by non-parallel sample surfaces. A soft spring is used in the load train (3000 N maximum force with 160 N/mm stiffness or 9000 N with 480 N/mm stiffness) to provide a relatively constant load when the sample expands under an electric field. Due to the spring and some heavy mechanical parts, only quasi-static measurements can be performed on this setup (< 1 Hz).

During measurements, a desired pre-stress is first applied to the sample and then an electric field is applied. The field-induced polarization is measured using a Sawyer-Tower circuit. The displacement of the sample is monitored by a linear variable differential transformer (LVDT), which is driven by a lock-in amplifier. By using a lock-in amplifier, the LVDT resolution is in the range of 10 nanometers. Note that the LVDT assembly is not part of the load train, but part of the steel frame. The LVDT is attached to a pair of micrometer-controlled positioning fixtures, which are fastened onto the steel frame. So when a sample strains under an electric field, the LVDT senses the relative motion between the frame and the top of the sample. During measurement, the sample is immersed in an insulating liquid, Fluorinert™ (3M, St. Paul, MN, USA), to prevent arcing. A heating ribbon assembly, which can be inserted into the liquid-filled Teflon™ cup, allows the sample temperature to reach as high as 165°C (Figure 2.2.2).

A major concern in this type of measurement is the friction at sample/fixture surfaces. Therefore, efforts were made to reduce the effects of frictional clamping. The contacts plates have a mirror finish with an average surface roughness of R_a = 5 nm. The clamping effect can be further reduced by using samples with high aspect ratio. Electrostrictive and antiferroelectric multilayer stacks with 10.0 mm diameter and 10.7 mm in height were built for the measurements. Each stack has 16 active layers which

have a thickness of 0.5 mm. Two passive endcaps at the top and bottom of the stack are made of the same material and were polished to R_a = 75 nm on the outer surfaces. The electrical contact of the discs is realized by 50 μm thick metal shims between the active layers. For the conventional PZT compositions, only pellets, approximately 13 mm in diameter and 1 mm in thickness, were tested due to limited powder quantity.
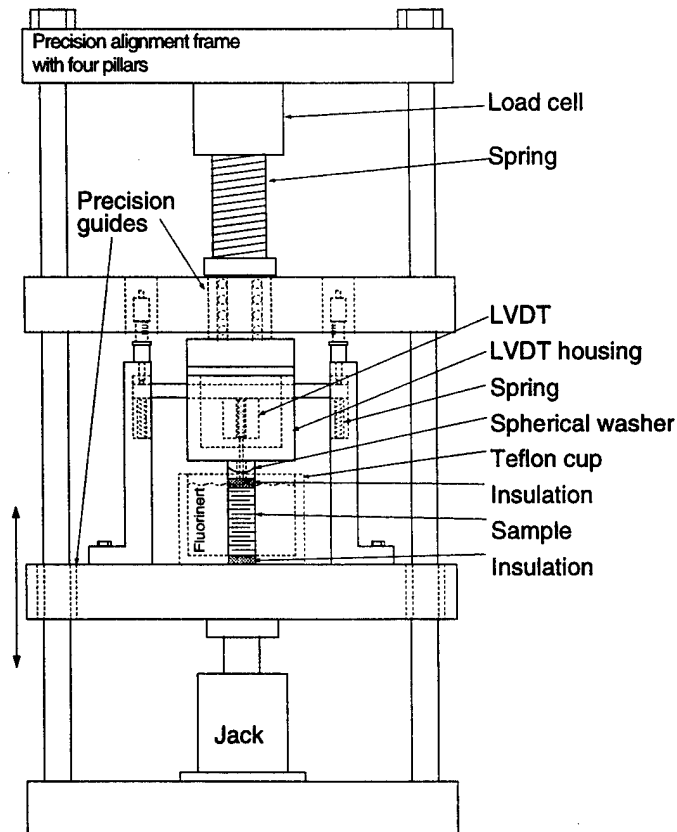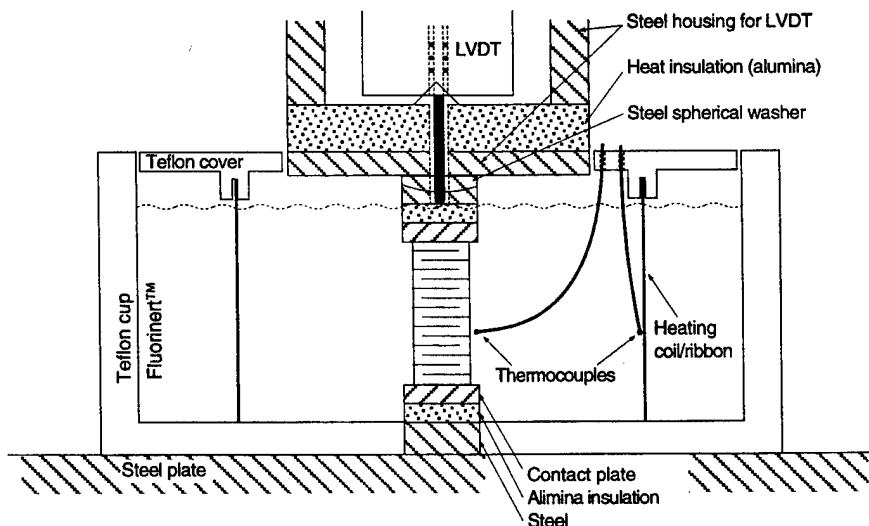

Figure 2.2.1 A schematic of the experimental setup for pre-stress measurements

Steel housing for LVDT

LVDT

Heat insulation (alumina)

Steel spherical washer

Teflon cover

Teflon cup

Fluorinert™

Heating coil/ribbon

Thermocouples

Steel plate

Contact plate
Alimina insulation
Steel

Figure 2.2.2 A schematic of the Teflon™ heating bath

2.3   ELECTROSTRICTIVE CERAMICS

Uniaxial stress up to 100 MPa was applied to various samples.   During the measurements, pre-stressed samples expand under the applied electric field and the corresponding polarization and displacement were measured simultaneously. Shown in Figures 2.3.1(a) and (b) is the stress dependence of PMN-PT 90-10. Only small changes in polarization and strain were observed. At 100 MPa, the material still retains 85% and 68% of its stress-free polarization and strain, respectively. The hysteresis remained virtually unchanged for all stresses.   Moreover, the strain versus polarization curves showed perfect parabolic shapes for all stresses (Figure 2.3.1c), indicating that the electrostrictive coefficient, Q_{111}, was independent of the applied stress. By using least square regression, the above coefficient was determined to be 0.0178 m^4/C^2.

PMN-PT 76-24 material, which has a higher dielectric maximum temperature due to its higher PT content, was tested at its operating temperature, 85°C. As shown in Figures 2.3.1(d) to (f), it had the same characteristics as PMN-PT 90-10, although its strain level was almost 50% higher than that of 90-10. This was not surprising because 76-24 is

simply the high temperature version of 90-10. The electrostrictive coefficient Q_{111}, which was determined to be 0.0210 m^4/C^2, was also independent of stress.

Both materials were also subjected to various combinations of temperature and stress. For each condition, a unipolar (half sine wave) electric field with a 20 kV/cm maximum was applied to the sample. The results for PMN-PT 90-10 are plotted in figures 2.3.2(a) and (b). This shows that the field-induced polarization and strain decreased monotonically with increasing temperature as it moves away from its dielectric maximum and into the paraelectric region. The stress dependence of 90-10 remained similar for all temperatures. PMN-PT 76-24 displays the same behavior at temperatures higher than 85°C. At room temperature, however, a stress dependence typical of a normal "soft" ferroelectric material was seen. The observed behavior was the result of two competing processes: domain flipping due to stress (polar direction perpendicular to stress) and electric field (polar direction align with field). Similar behavior of soft piezoelectrics has been reported in the past.
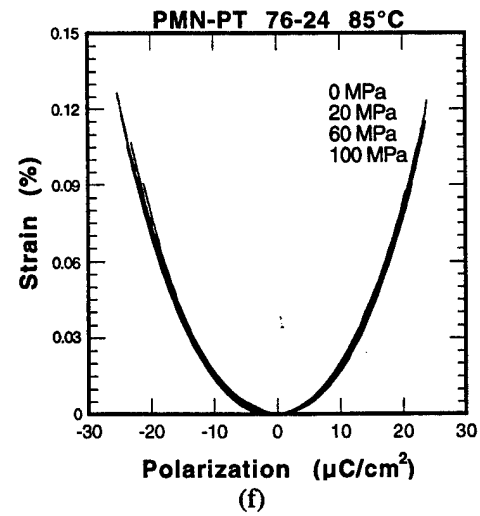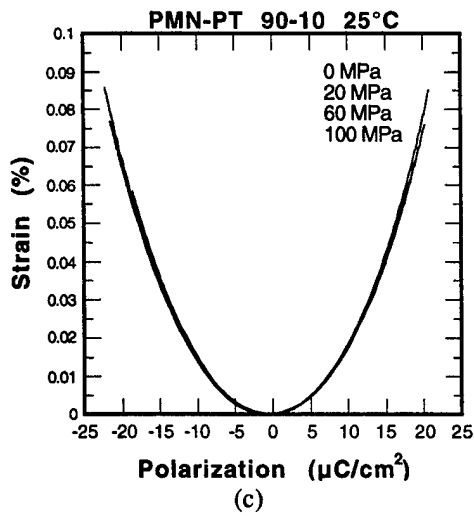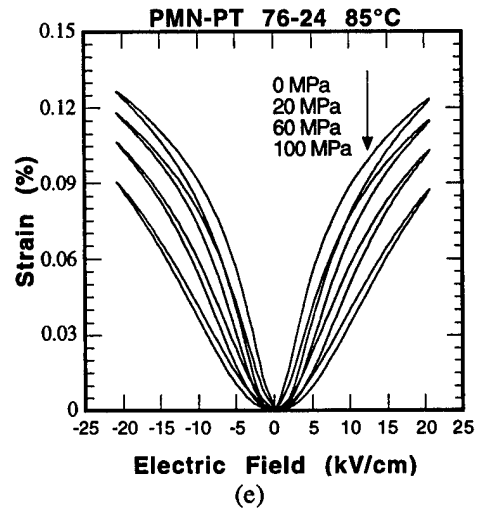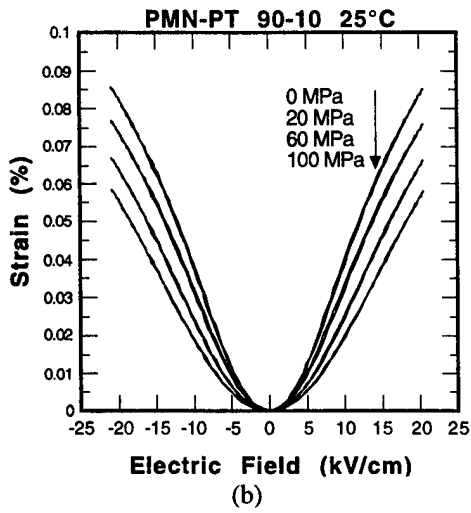
PMN-PT 90-10 25°C

Polarization (μC/cm²) vs Electric Field (kV/cm)

0 MPa
20 MPa
60 MPa
100 MPa

(a)

PMN-PT 76-24 85°C

Polarization (μC/cm²) vs Electric Field (kV/cm)

0 MPa
20 MPa
60 MPa
100 MPa

(d)

PMN-PT 90-10 25°C

Strain (%) vs Electric Field (kV/cm)

0 MPa
20 MPa
60 MPa
100 MPa

(b)

PMN-PT 76-24 85°C

Strain (%) vs Electric Field (kV/cm)

0 MPa
20 MPa
60 MPa
100 MPa

(e)

PMN-PT 90-10 25°C

Strain (%) vs Polarization (μC/cm²)

0 MPa
20 MPa
60 MPa
100 MPa

(c)

PMN-PT 76-24 85°C

Strain (%) vs Polarization (μC/cm²)

0 MPa
20 MPa
60 MPa
100 MPa

(f)
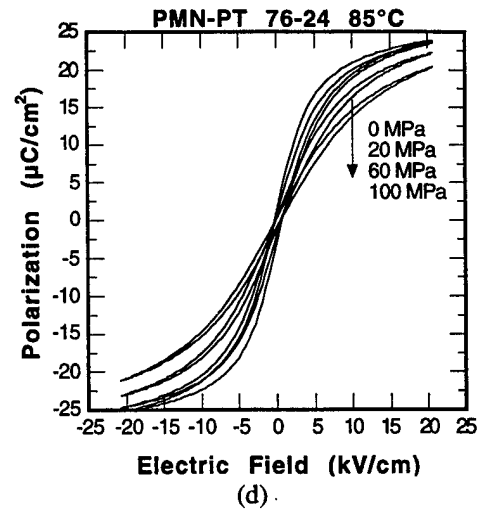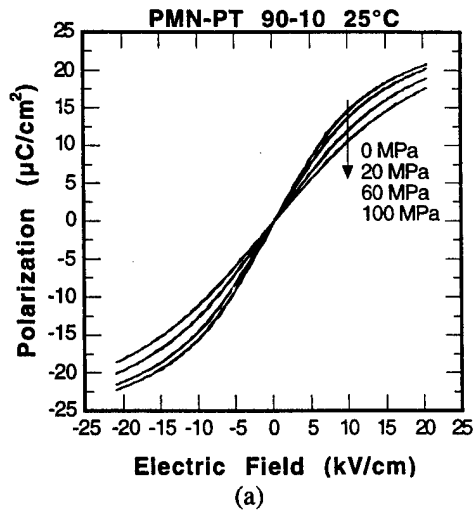
Figure 2.3.1   The polarization and strain behaviors of PMN-PT 90-10 ((a)-(c)) and 76-24 ((d)-(e))
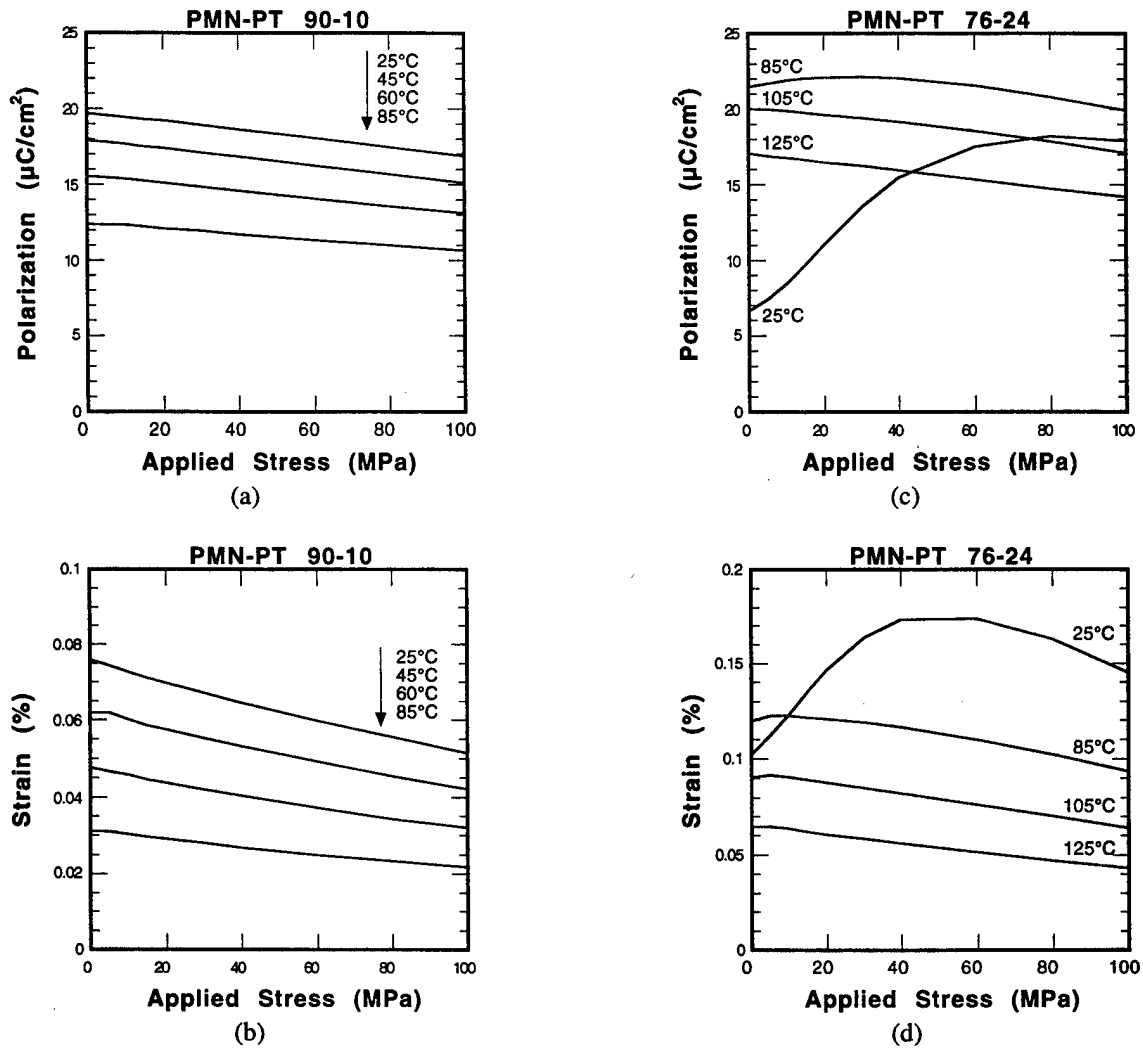
Figure 2.3.2   The polarization and strain of PMN-PT 90-10 and 76-24 under various
combination of temperature and stress

2.2.4   PHASE SWITCHING CERAMICS

Like the electrostrictive materials, uniaxial stress up to 100 MPa was applied to the phase
switching material.   Some of the results are shown in Figure 2.4.1. It is interesting to
observe that the overall strain increases with increasing pre-stress. As shown in Figure
2.4.2(a), the strain at stresses greater than 80 MPa can be twice as high as that without

pre-stress. At the same time, however, the polarization remained relatively unchanged, indicating that the AFE-to-FE phase switching was complete. Apparently, there was a decoupling between the polarization and strain. The pre-stress also increased the switching fields as shown in Figure 2.4.2(b). Both the forward and backward switching fields have equivalent slopes of 0.11 kV/cm per MPa. The hysteresis (the difference between the forward and backward switching fields) remained constant at about 20 kV/cm.

To explain the above observations of phase switching behavior under uniaxial stress, we propose an addition to the following switching sequence, as illustrated in Figure 2.4.3. It is possible that the AFE domains of a typical electric field-exposed sample (b) collapse under applied stress (b'). This makes the sample smaller in the stress direction. As a result, the dimensional change in E-field direction between the AFE and FE states (b' to e) of a stressed sample is larger than that of a stress-free sample (b to e). The collapsed AFE domain state also implies that additional energy is needed during phase transformation when a sample stretches against the applied stress, which explains why the increased switching field under stress. Experimental confirmation of the proposed explanation, however, is still needed.

Finally, it was noted that the strain of multilayer samples, even without external stress, is more than 30% smaller than that of a single pellet (Fig. 2.4.2a). This reduction in performance was likely due to the multilayer structure. Specifically, the passive endcaps, shims and epoxy used for assembling the multilayer stacks constrain the active ceramic layers expansion in the transverse directions and caused a reduction of the longitudinal strain.

The effects of temperature on phase switching were also examined. Because the epoxy used for assembling the antiferroelectric multilayer stacks does not have high temperature capability, the measurements were performed only at 50 and 75 °C. Table IV is the summary of the strain and hysteresis under various stresses and temperatures. The strain showed a remarkable stability for the temperature range 20 to 75°C. At 60 MPa, the

strain at 75°C retained more than 75% of the strain at 21°C. This composition also displayed reduced hysteresis at higher temperatures.
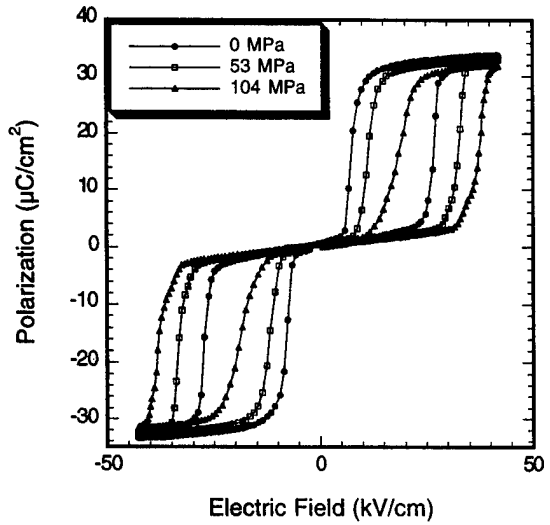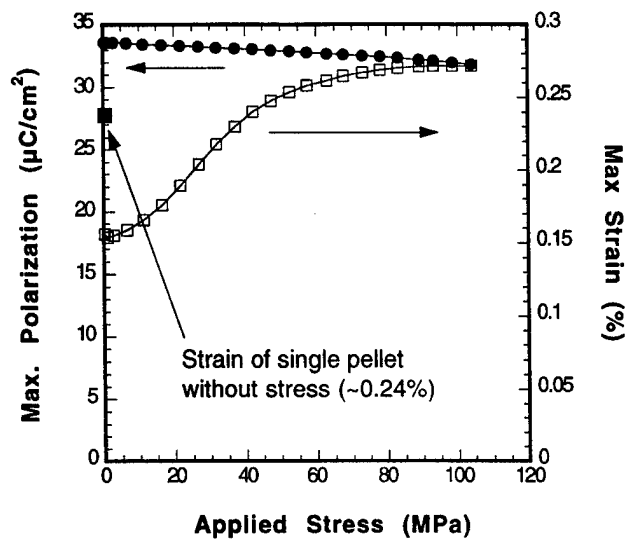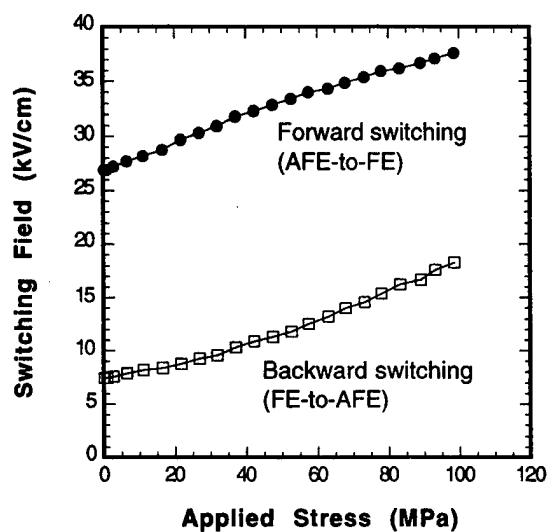

(a)
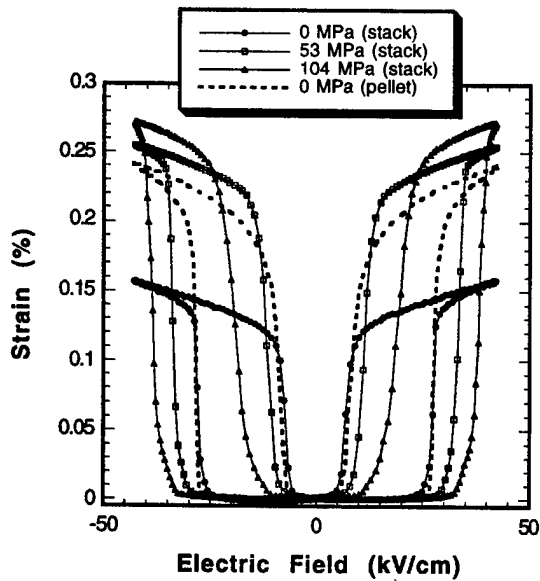
(b)

Figure 2.4.1 (a) Polarization and (b) strain behaviors under various pre-stresses

(a)

(b)

Figure 2.4.2   (a) Maximum polarization and strain and (b) switching fields as a function of pre-stress for the PLSnZT antiferroelectric material
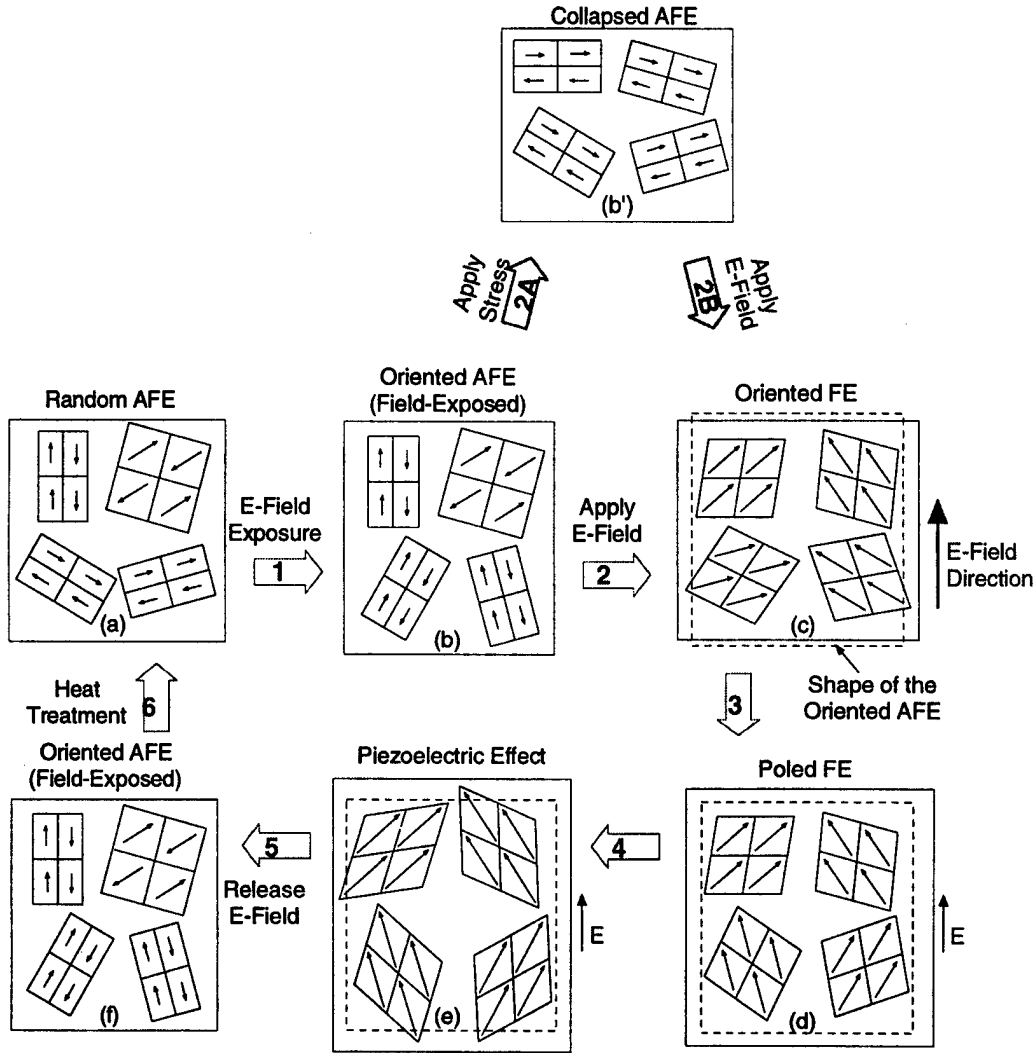
Figure 2.4.3   A schematic of the AFE-FE phase switching steps. The proposed extra steps 2A and 2B are caused by the uniaxial stress.

Table IV   The strain and hysteresis at various stresses and temperatures of the antiferroelectric material in this study

	Strain (%)		Hysteresis (kV/cm)	
	0 MPa	60 MPa	0 MPa	60 MPa
21°C	0.144	0.252	21.3	21.0
50°C	0.137	0.230	14.3	15.0
75°C	0.124	0.191	9.1	9.5

2.5 CONVENTIONAL PZTs

Figure 2.2.5.1 shows the polarization as a function of electric field for 2.4% Nb-doped PZT 56/44, 52/48 and 48/52 ceramics with and without PbO compensation. The remnant polarization (P_r), coercive field (E_c) and longitudinal piezoelectric coefficient (d_{33}) are listed in Table V.

Table V P_r, E_c and d_{33} of PZT 56/44, 52/48 and 48/52 with and without PbO compensation.

	Without PbO excess			With 3% PbO excess		
	Pr (μC/cm2)	Ec (kV/cm)	d33* (pC/N)	Pr (μC/cm2)	Ec (kV/cm)	d33* (pC/N)
PZT 56/44	42.5	10.8	243	43.3	11.0	250
PZT52/48	38.7	17.8	364	40.7	14.5	400
PZT48/52	30.7	27.6	160**	34.6	25.1	---**

* Samples were poled at 120°C with electric fields which were 3- 4 times of E_c. d_{33} were measured by d_{33} meter.
**Sample breakdown.

The strain as a function of electrical field for Nb-doped PZT 52/48 and 48/52 ceramics with and without PbO compensation is shown in Figure 2.5.2. Under a fixed electrical field, the sample with PbO compensation showed higher strain relative to samples without PbO compensation.

Figure 2.5.3 shows the strain as a function of electrical field for Nb-doped PZT 56/44, 52/48 and 48/52 with PbO compensation. It is evident that the morphotropic phase boundary composition, i.e. PZT 52/48, exhibits highest strain under electrical field relative to PZT 56/44 and PZT 48/52.

The baseline properties PZT 56/44, 52/48 and 48/52 ceramics were characterized using resonance methods. The results are consistent with that of previously reports. Table VI summarizes the electrical properties of the samples studied using various methods.
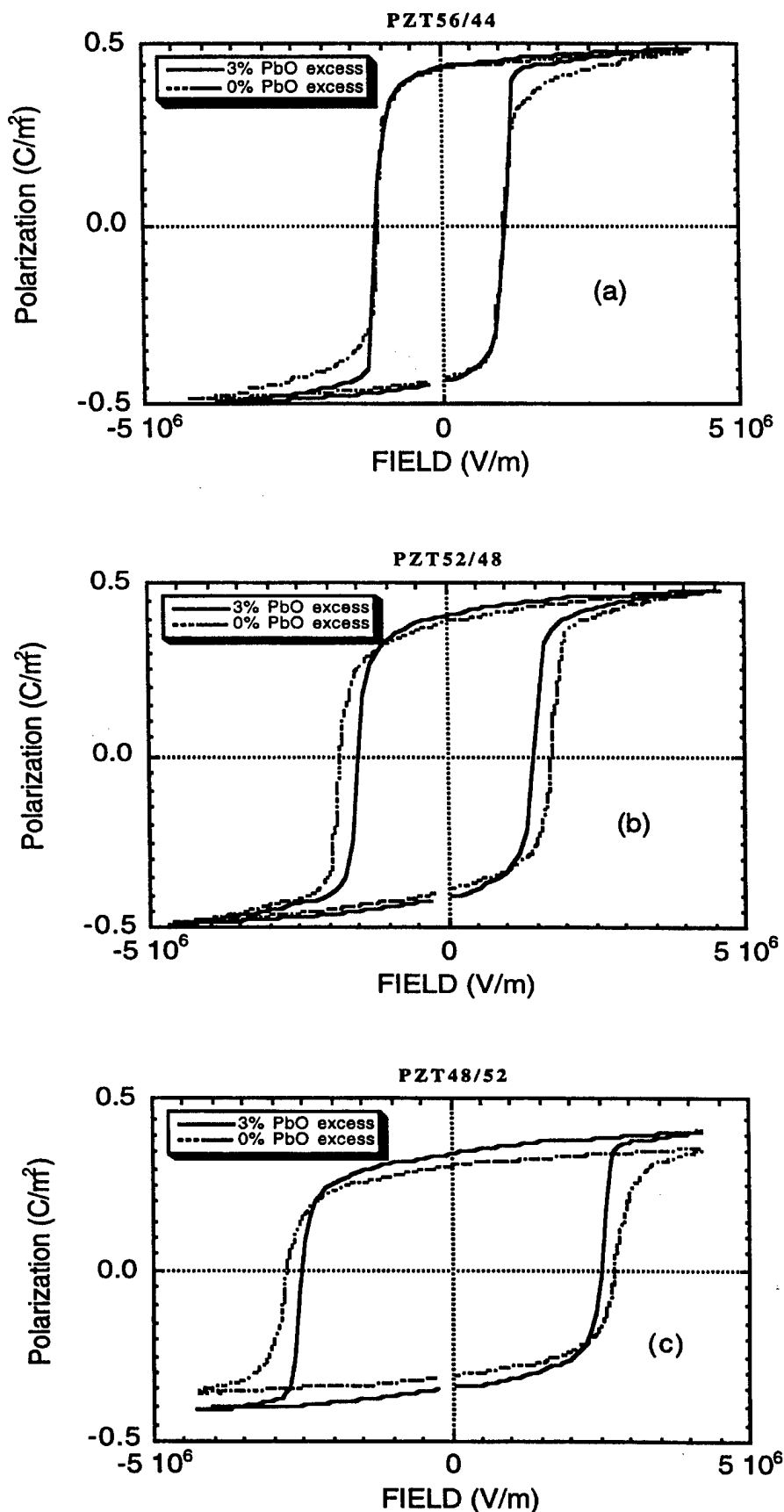
Figure 2.5.1 Ferroelectric hysteresis loops of 2.4% Nb-doped (a) PZT 56/44, (b) 52/48, and (c) 48/52 ceramics with (solid lines) and without (dashed lines) PbO compensation.
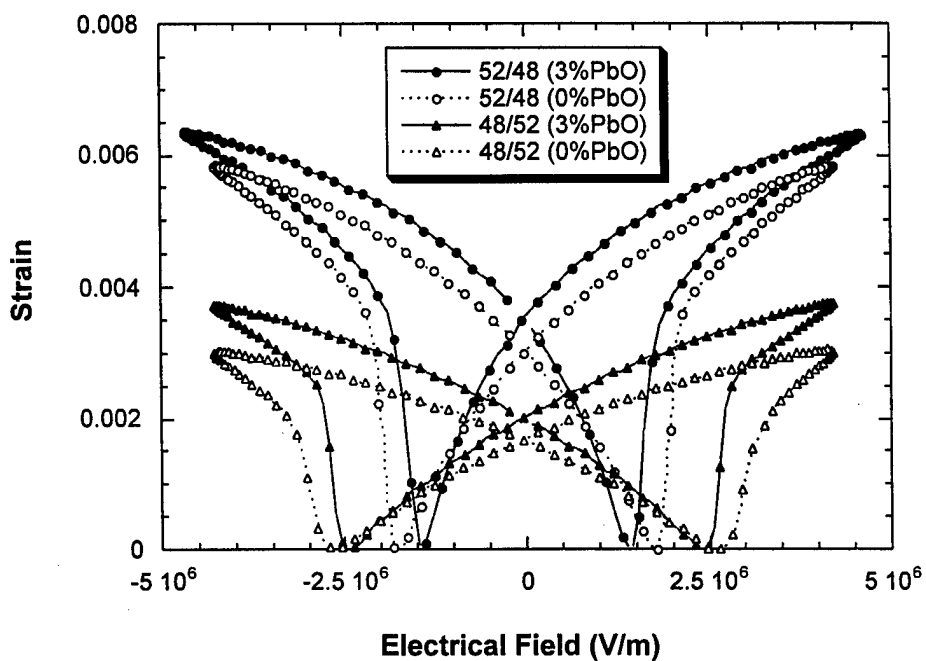
Figure 2.5.2 Strain as a function of electric field for PZT 52/48 and PZT48/52 ceramics with and without PbO compensation.
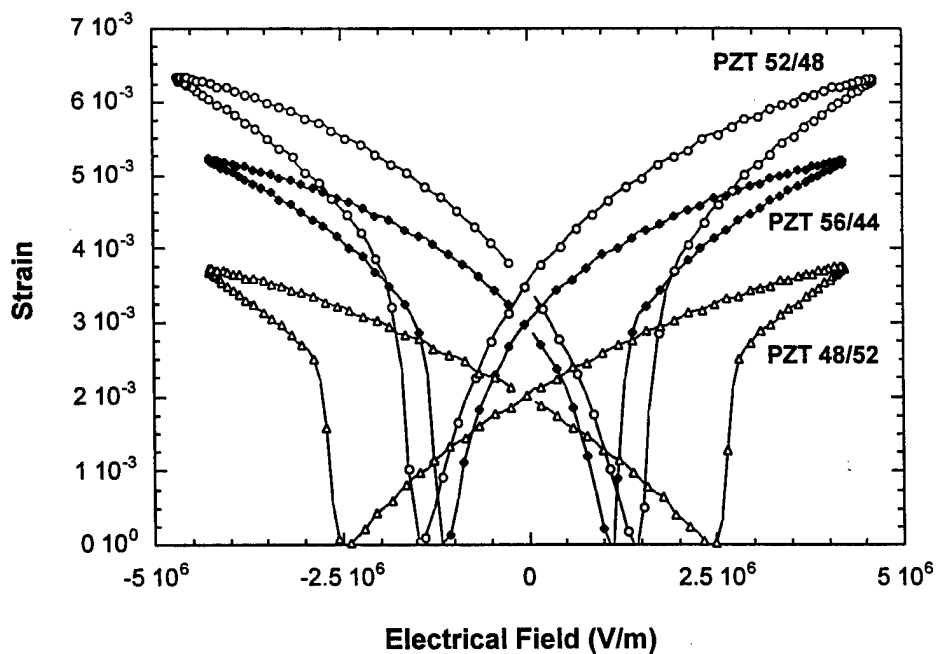

Figure 2.5.3 Strain as a function of electric field for PZT56/44, PZT 52/48 and PZT 48/52 ceramics with PbO compensation.

Table VI Electrical properties of PZT 56/44, 52/48 and 48/52 characterized using various methods.

	PZT56/44	PZT52/48	PZT48/52	Note
Density (g/cm^3)	7.83	7.83	7.86	
ε (poled)	796.7	1651.4	1147.0	120C/10min at 2Ec Measured at f = 1 (kHz)
tgδ (poled)	0.027	0.018	0.013	120C/10min at 2Ec Measured at f = 1 (kHz)
ε (unpoled)	1338.5	1633.3	1070.2	f = 1 (kHz)
tgδ (unpoled)	0.03	0.02	0.016	f = 1 (kHz)
Pr (μC/cm^2)	43.3	40.7	34.6	f = 1 (Hz)
Ec (kV/cm)	11.1	14.5	25.1	f = 1 (Hz)
d_{33} (pC/N)	234	406	247	Berlincout meter
d_{31} (pC/N)	97.6	167.3	98.5	Resonance method
σ (Poisson's ratio)	0.305	0.403	0.403	Resonance method
k_p (Planar)	0.57	0.62	0.50	Resonance method
k_{31} (Transverse)	0.34	0.34	0.27	Resonance method
s_{11} (m^2/N)	1.2×10^{-11}	1.7×10^{-11}	1.3×10^{-11}	Resonance method
Q Mech. Quality	78.7	99.5	145.6	Resonance method

The ceramic samples can be poled at 120°C with an electrical field equal to 3 times the coercive field. Addition of 3% PbO increases the density of the sintered samples, slightly increases the d_{33} value and decreases the coercive field. A more square electrical hysteresis loop is observed on PbO compensated PZT ceramics. The electrical properties of the prepared samples are consistent with what have been published previously.

2.5.1 PZT 56/44:

1) 2.4% Nb doping with 3% PbO compensation

2) Structure: Rhombohedral.

3) Unipolar sinusoidal electric field.

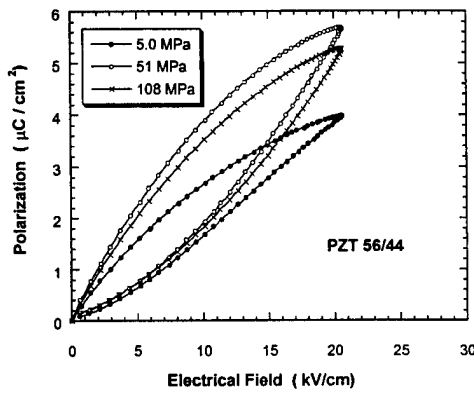4) Frequency: 1 Hz. Temperature: room temperature.

Figure 2.5.4a. Polarization as a function of electric field for PZT 56/44 ceramics at various DC uni-axial stresses.
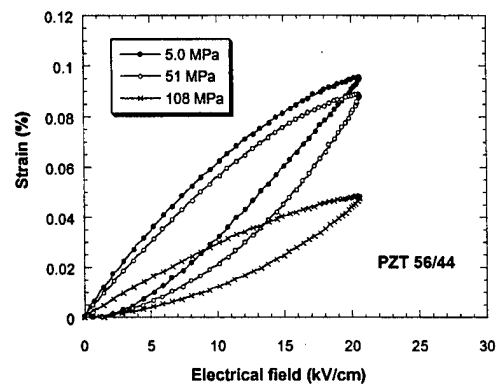

Figure 2.5.4b. Strain as a function of electric field for PZT56/44 ceramics at various DC uni-axial stresses.
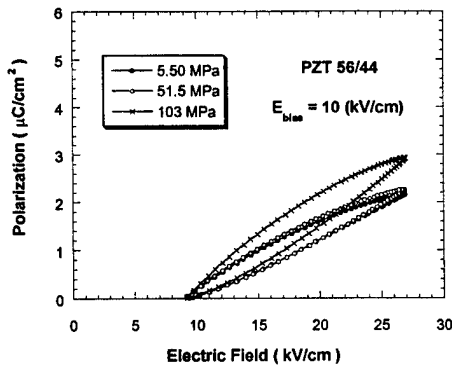

Figure 2.5.5a. Polarization as a function of electric field for PZT 56/44 at various DC stresses measured under 10kV/cm DC electric bias.
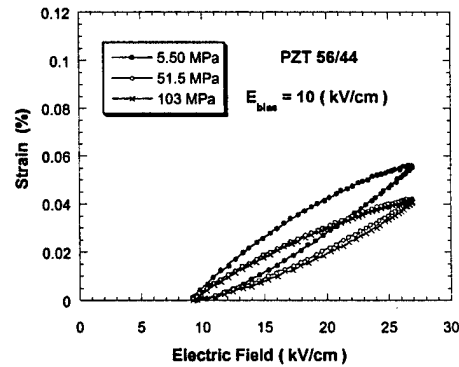

Figure 2.5.5b. Strain as a function of electric field for PZT 56/44 at various DC stresses measured under 10kV/cm DC electric bias.

27

Figure 2.5.4 shows a) polarization (P), b) strain (S) as a function of electric field (E) for PZT 56/44 ceramics. The P-E loop under 5.0 MPa stress shown in figure 2.5.4a is slimmer than those observed under 51 and 108 MPa stresses. The maximum polarization that is observed at 5.0 MPa stress is lower than those obtained at 51 and 108MPa stresses. These might be due a de-poling effect during the measurement. It has been shown in the previous section that the coercive field of PZT 56/44 ceramics is rather low, indicating that the ferroelectric domains are easily switched. The application of a high dc stress may reorient the originally aligned ferroelectric domains. When the measurement signal is applied to the sample, the reoriented domains are poled again. Therefore, an increased polarization will be observed. The S-E loops behave differently. The maximum strain decreases with increasing DC stress.

In order to clarify the de-poling effect during the measurement, the polarization and strain as a function of electric field for PZT 56/44 ceramics were measured under 10kV/cm DC electric bias (shown in Figure 2.5.6a and b respectively). It can be seen that the P-E loops are much slimmer than those observed under 0 electric bias. The maximum polarization obtained at low DC stress is lower than those observed under high stresses. The S-E loops are also much slimmer.

Figure 2.5.6a. Maximum polarization as a function of uni-axial stress for PZT 56/44 measured under 0 and 10kV/cm electric bias.

Figure 2.5.6b. Maximum strain as a function of uni-axial stress for PZT 56/44 measured under 0 and 10kV/cm electric bias.
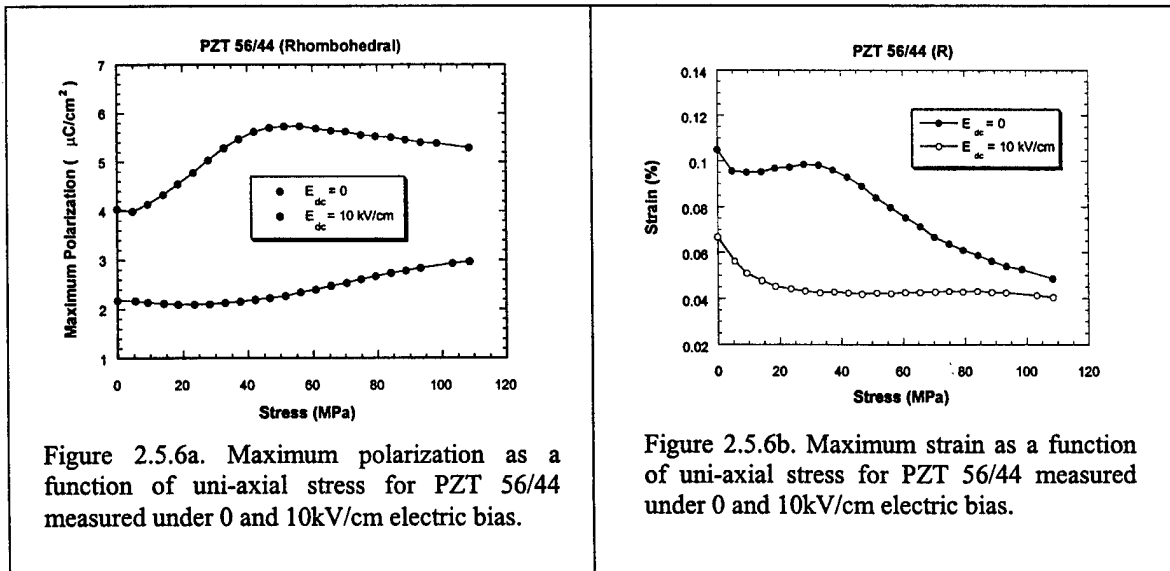
Figure 2.5.6 compares a) polarization and b) strain as a function of stress for PZT 56/44 ceramics measured under 0 and 10 kV/cm electric bias. Under 0 bias, PZT 56/44 has an

explicit de-poling effect during the P-E and S-E measurements. Under DC electric bias, say 10kV/cm, the de-poling effect is depressed which is evidenced by the more stable stress dependence of polarization and strain.

2.5.2 PZT 52/48:

1) 2.4% Nb doping with 3% PbO compensation.
2) Structure: Rhombohedral + Tetragonal
3) Unipolar sinusoidal electric field.
4) Frequency: 1 Hz. Temperature: room temperature.

Figure 2.5.7a and Figure 2.5.8a show the polarization as a function of electric field for PZT 52/48 ceramics at various stresses measured under 0 and 10kV/cm electric bias. It can be seen that the P-E loops in both cases are not changing with the variation of applied stress. The maximum polarization (shown in Figure 2.5.9a) is almost independent of stress in both cases, indicating that there is no de-poling effect in this composition. The relatively high coercive field of this composition may be responsible for the stable stress dependence of polarization.

The strain (S) vs. electric field (E) changes dramatically with increasing applied stress as shown in Figure 2.5.7b and Figure 2.5.8b. The fact that S-E loop becomes very large under low stresses indicates a strong extrinsic contribution to the piezoelectrically-induced strain. The non-180° domains, which are difficult to be aligned, reorient after the removal of the poling field. Those domains can be driven by the applied unipolar electric field, giving rise to an addition contribution to the piezoelectrically induced strain. A high stress on the sample may clamp the vibration of those non-180° domain walls resulting in a slimmer S-E loop and lower strain. The application of the electric bias may keep some of the non-180° domain aligned on the direction of the bias field. Therefore, a lower
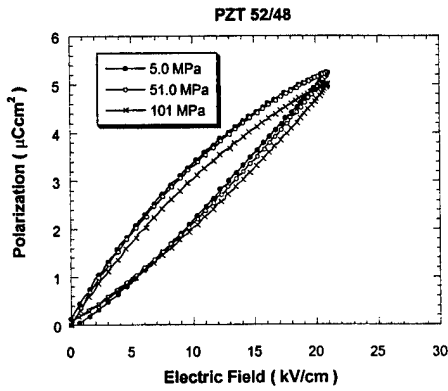
Figure 2.5.7a. Polarization as a function of electric field for PZT 52/48 ceramics under various DC uni-axial stresses.
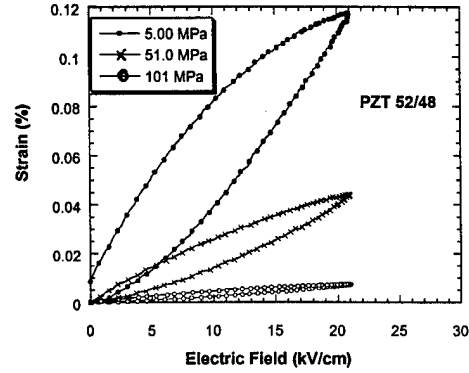
Figure 2.5.7b. Strain as a function of electric field for PZT 52/48 ceramics under various DC uni-axial stresses.
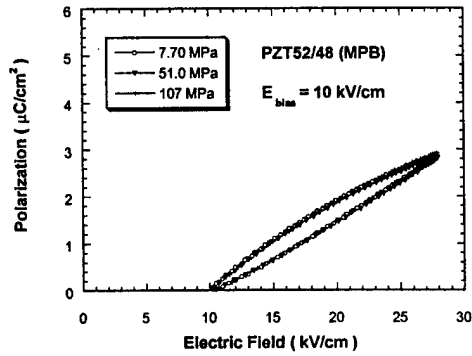
Figure 2.5.8a. Polarization as a function of electric field for PZT 52/48 at various DC stresses measured under 10kV/cm DC electric bias.
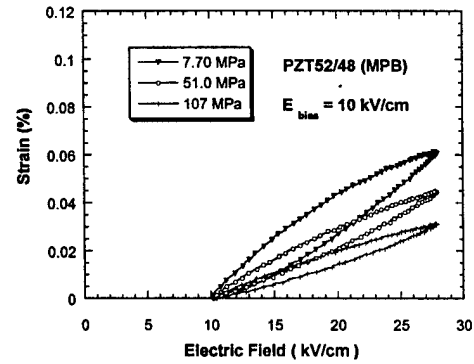
Figure 2.5.8b. Strain as a function of electric field for PZT 52/48 at various DC stresses measured under 10kV/cm DC electric bias.
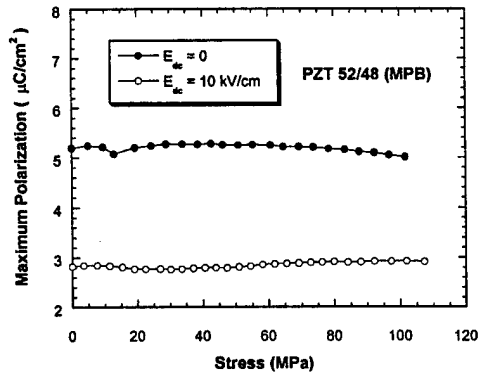
Figure 2.5.9a. Maximum polarization as a function of uni-axial stress for PZT 52/48 measured under 0 and 10kV/cm electric bias.
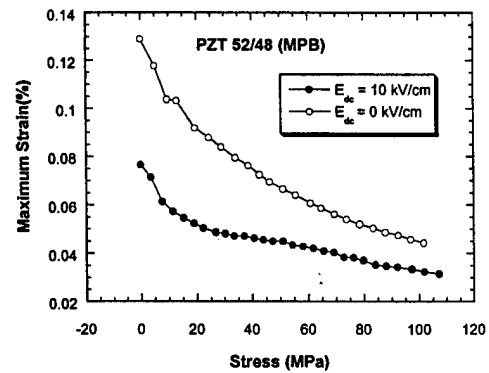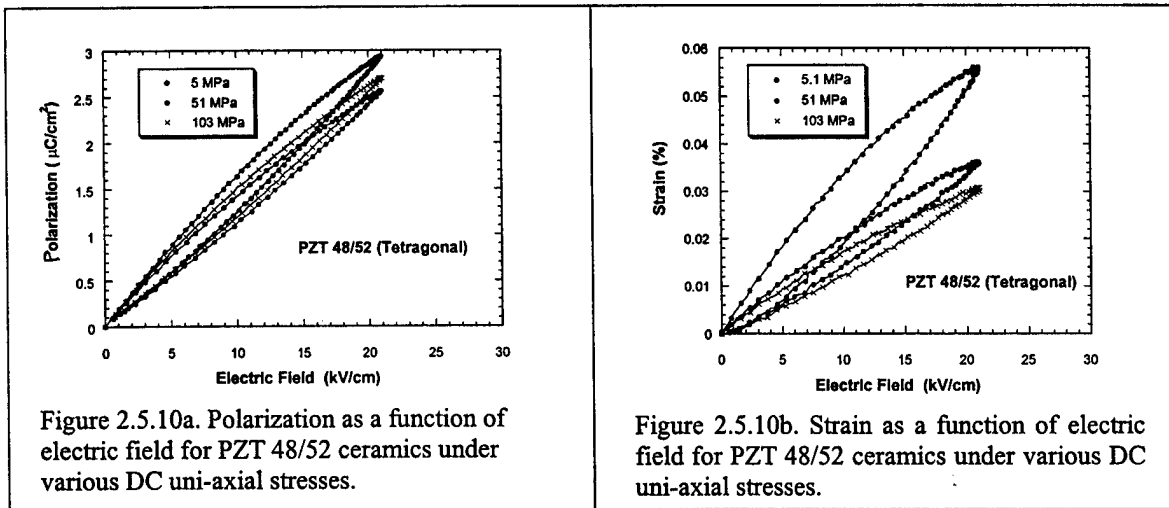
Figure 2.5.9b. Maximum strain as a function of uni-axial stress for PZT 52/48 measured under 0 and 10kV/cm electric bias.

30

maximum strain (Figure 2.5.9b) and a slimmer S-E loop (Figure 2.5.8b) will be obtained for the samples under bias.

2.5.3   PZT 48/52:

1) 2.4% Nb doping with 3% PbO compensation.

2) Structure: Rhombohedral + Tetragonal

3) Unipolar sinusoidal electric field.

4) Frequency: 1 Hz. Temperature: room temperature.

Tetragonal PZT (PZT 48/52) showed much slimmer P-E loops (Figure 2.5.10a and Figure 2.5.11a). The stress dependence of maximum polarization is rather stable, and a 10kV/cm bias field can make the polarization almost independent of stress (Figure 2.5.11a). The high coercive field of this composition may be the reason for the stable stress dependence of polarization.

Figure 2.5.10a. Polarization as a function of electric field for PZT 48/52 ceramics under various DC uni-axial stresses.

Figure 2.5.10b. Strain as a function of electric field for PZT 48/52 ceramics under various DC uni-axial stresses.
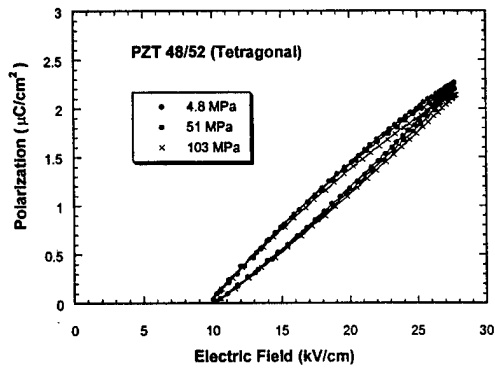
Figure 2.5.10a. Polarization as a function of electric field for PZT 48/52 at various DC stresses measured under 10kV/cm DC electric bias.
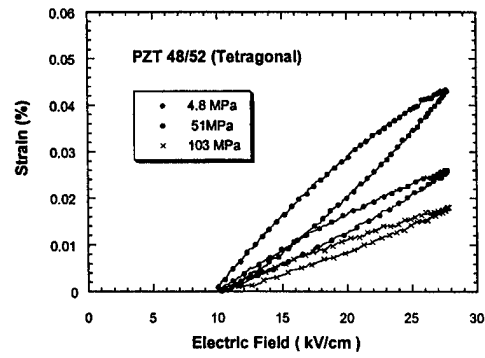

Figure 2.5.10b. Strain as a function of electric field for PZT 48/52 at various DC stresses measured under 10kV/cm DC electric bias.
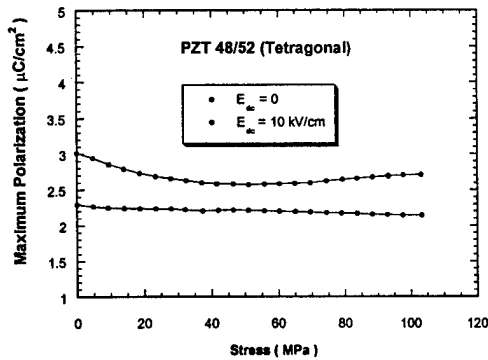

Figure 2.5.11a. Maximum polarization as a function of uni-axial stress for PZT 48/52 measured under 0 and 10kV/cm electric bias.
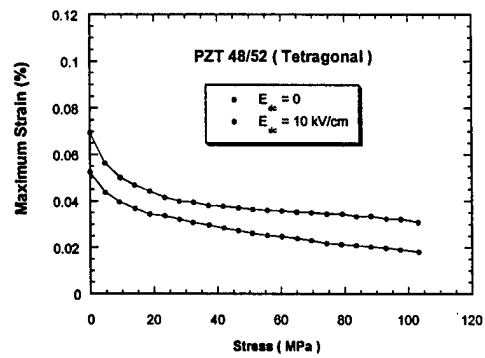

Figure 2.5.11b. Maximum strain as a function of uni-axial stress for PZT 48/52 measured under 0 and 10kV/cm electric bias.

The stress dependence of strain showed similar behavior as that of PZT 52/48. The application of bias did not change the trend of maximum strain vs. stress but lowered the observed strain in general.

2.6 Summary and Conclusions

An experimental setup that applies up to 9000 N of uniaxial force was designed and built. This apparatus provided an easy way to load/unload samples and to conduct experiments. Extra caution was taken to prevent any transverse movement or bending on samples. The clamping effect at contact surfaces was reduced by using mirror finish contact plates.

The effect can be further reduced by using high aspect ratio samples, i.e., multilayer stacks.

For electrostrictive ceramics, PMN-PT 90-10 and its high temperature (85°C) counterpart 76-24, were tested. It was shown that neither electrostrictive PMN-PT is sensitive to external stress, while 76-24 showed superior electromechanical properties to 90-10. The electrostrictive coefficients for both materials were independent of stress. PMN-PT, nevertheless, was very sensitive to temperature change, because it was mostly operated at temperatures near its dielectric maximum. For the antiferroelectric material in this study, the strain at high pre-stress (>80 MPa) was almost twice as high as the strain without pre-stress. This is likely due to the AFE domain re-orientation process under load. The material also showed excellent stability in performance for the temperature range 20 to 75°C under various pre-stresses.

PZT materials are prone to ferroelectric domain reorientation under uniaxial stress. The rhombohedral composition 56/44, which has the smallest coercive field among the three, had the largest stress dependence, owing to easy depoling under stress. This depoling effect, however, can be reduced by keeping an electric field bias on the sample to suppress domain motion. On the other hand, the tetragonal PZT 48/52 was much less stress dependent. The constant polarization under all stresses showed that there was no/little depoling effect. The strain behavior indicated a strong extrinsic contribution to the piezoelectrically induced strain. The results allowed us to draw correlations between intrinsic material factors and external stresses, both mechanical and electrical.

Appendix

The Effects of Uniaxial Stress and Temperature

on the Behavior of Antiferroelectric Ceramics

Patrick Pertsch
Fraunhofer-Institute for Applied Optics and Precision Engineering, D-07745 Jena, Germany

Ming-Jen Pan, Fan Chu, and Shoko Yoshikawa
Materials Research Laboratory, The Pennsylvania State University, University Park, PA 16802
USA

Abstract—In this study the effects of pre-stress and temperature on a lead lanthanum stannate zirconate titanate (PLSnZT) composition were examined, with an emphasis on the phase transformation behavior. An experimental setup capable of applying 9000 N of uniaxial stress was carefully designed such that the clamping effect due to sample/fixture contacts is minimized. With this setup, both the polarization and displacement under a quasi-static electric field can be measured simultaneously at different temperatures. Interestingly, the overall strain of the PLSnZT composition increases with increasing uniaxial stress. This might be the result of re-orientation of antiferroelectric domains under pre-stress. The composition also showed excellent stability in strain over the temperature range 20 to 75°C under stress as high as 100 MPa.

PACS No: 77.80.Fm, 62.20.–x, 81.40.–z, 77.80.Dj

I. INTRODUCTION

The lead lanthanum stannate zirconate titanate (PLSnZT) system has been widely studied for actuator applications. In this family of ceramics, the antiferroelectric tetragonal (AFE_{tet}) phase can be readily switched to its neighboring ferroelectric rhombohedral (FE_{rh}) phase with the application of an electric field. This phase transition is accompanied with a large change in volume associated with high longitudinal strain (in the field direction). Crystallographic analyses based on X-ray diffraction have shown that 0.5% is the maximum strain possible for an ideal single crystal in this system [1,2].

Actuator materials are often used under large mechanical load or placed in pre-stressed conditions to maintain their integrity during service. In addition, actuators are often used in encapsulated environment where heat dissipation might cause local temperature increase. As a result, there have been a lot of interest in studying actuator response under pre-stress and temperature. Previous studies mostly have focused on the piezoelectric properties of various ferroelectrics under uni-axial stress. Unlike piezoelectric materials which only involve ferroelectric domain reorientation, antiferroelectric materials also undergo a phase transition and change in unit cell dimensions. In this study, we intended to emphasize how the pre-stress affect the antiferroelectric-to-ferroelectric (AFE-FE) phase switching behavior.

This report investigates the behavior of PLSnZT ceramics under pre-stress. A composition in the AFE_{tet} region, $(Pb_{0.98}La_{0.02})(Sn_{0.33}Zr_{0.55}Ti_{0.12})_{0.995}O_3$, was chosen for this study.

II. EXPERIMENTAL SETUP AND SAMPLES

An experimental setup was designed to measure the material and actuator response under both uniaxial stress and temperature (Fig. 1). A rigid, precisely guided steel frame provides true uniaxial stress during loading. The spherical washer on top of the upper contact plate further minimizes transverse force and bending moment caused by non-parallel sample surfaces.

A soft spring is used in the load train (3000 N maximum force with 160 N/mm stiffness or 9000 N with 480 N/mm stiffness) to provide relative constant load when the sample expands under an electric field. Due to the spring and the some heavy mechanical parts, only quasi-static measurements can be performed on this setup (< 1 Hz). The displacement of the sample is monitored by a linear variable differential transformer (LVDT), which is driven by a lock-in amplifier. During measurement, the sample is immersed in an insulating liquid Fluorinert™ (3M, St. Paul, MN, USA) to prevent arcing. A heating ribbon assembly, which can be inserted into the liquid-filled Teflon cup, allows the sample temperature to reach as high as 165°C.

Efforts were made to reduce the effects of clamping at sample/fixture contact surfaces. The contacts plates have a mirror finish with an average surface roughness of $R_a = 5$ nm. The clamping effect can be further reduced by using samples with high aspect ratio. In this study multilayer stacks with 10.0 mm diameter and 10.7 mm in height are built for the measurements. Each stack has 16 active layers which have a thickness of 0.5 mm. Two passive endcaps at the top and bottom of the stack are made of the same material and were polished to $R_a = 75$ nm on the outer surfaces. The electrical contact of the discs is realized by 50 μm thick metal shims between the active layers.

III. RESULTS AND DISCUSSION

Uniaxial stress up to 100 MPa was applied to various samples. During the measurements, pre-stressed samples expand under the applied electric field and the corresponding polarization and displacement were measured simultaneously. Some of the results are shown in Figure 2. It is interesting to observe that the overall strain increases with increasing pre-stress. As shown in Figure 3a, the strain at stresses greater than 80 MPa can be twice as high as that without pre-stress. At the same time, however, the polarization remained relatively unchanged, indicating that the AFE-to-FE phase switching is complete. Apparently, there is a decoupling between the polarization and strain. The pre-stress also increases the switching fields as shown in Figure 3b.

Both the forward and backward switching fields show a slope of 0.11 kV/cm per MPa. The hysteresis remained constant at about 20 kV/cm.

To explain the above observations of phase switching behavior under uniaxial stress, we propose an addition to the switching sequence in Reference 3, as illustrated in Figure 4. It is possible that the AFE domains of a typical electric field-exposed sample (b) collapse under applied stress (b'). This makes the sample smaller in the stress direction. As a result, the dimensional difference in E-field direction between the AFE and FE states (b' to e) of a stressed sample is larger than that of a stress-free sample (b to e). The collapsed AFE domain state also implies that additional energy is needed during phase transformation when a sample stretches against the applied stress, and thus the increased switching field under stress. Experimental confirmation of the proposed explanation, however, is still needed.

Finally, it was noted that the strain of multilayer samples, even without external stress, is more than 30% smaller than that of a single pellet (Fig. 3a). Apparently, this reduction in performance was due to the multilayer structure. Specifically, the passive endcaps, shims and epoxy used for assembling the multilayer stacks constrain the active ceramic layers expansion in the transverse directions and cause a reduction of the longitudinal strain.

The effects of temperature on phase switching were also examined. Because the epoxy used for assembling the multilayer stacks does not have high temperature capability, the measurements were performed only at 50 and 75 °C. Table I is the summary of the strain and hysteresis under various stresses and temperatures. The strain of composition A1 showed a remarkable stability for the temperature range 20 to 75°C. At 60 MPa, the strain at 75°C retained more than 75% of the strain at 21°C. This composition also showed reduced hysteresis at higher temperature.

IV. SUMMARY

An experimental setup that applies up to 9000 N of uniaxial force was designed and built. Extra caution was taken to prevent any transverse movement or bending on samples. The clamping effect at contact surfaces was minimized by using mirror finish contact plates and high aspect ratio samples, i.e., multilayer stacks. The strain at high pre-stress (>80 MPa) is almost twice as high as the strain without pre-stress. This is likely due to the AFE domain re-orientation process under load. The material also showed excellent stability in performance for the temperature range 20 to 75°C under various pre-stresses.

V. REFERENCES

[1] C.T. Blue, J.C. Hicks, S.-E. Park, S. Yoshikawa, and L.E. Cross, "*In situ* X-Ray Diffraction Study of the Antiferroelectric-ferroelectric Phase Transition in PLSnZT," *Appl. Phys. Lett.*, **68** [21] 2942-44 (1996).

[2] L. Shebanov, M. Kusnetsov, and A. Sternberg, "Electric Field-Induced Antiferroelectric-to-Ferroelectric Phase Transition in Lead Zirconate Titanate Stannate Ceramics Modified with Lanthanum," *J. Appl. Phys.*, **76** [7] 4301-4 (1994).

[3] S.-E. Park, M.-J. Pan, K. Markowski, S. Yoshikawa, and L.E. Cross, "Electric Field Induced Phase Transition of Antiferroelectric Lead Lanthanum Zirconate Titanate Stannate Ceramics," *J. Appl. Phys.*, **82** [4] 1798 (1997).

FIGURE CAPTIONS

Figure 1 The experimental setup for pre-stress measurements

Figure 2 (a) Polarization and (b) strain behaviors under various pre-stresses.

Figure 3 (a) Maximum polarization and strain and (b) switching fields as a function of pre-stress

Figure 4 A schematic showing the AFE-FE phase switching steps. The proposed extra steps 2A and 2B are caused by the uniaxial stress.
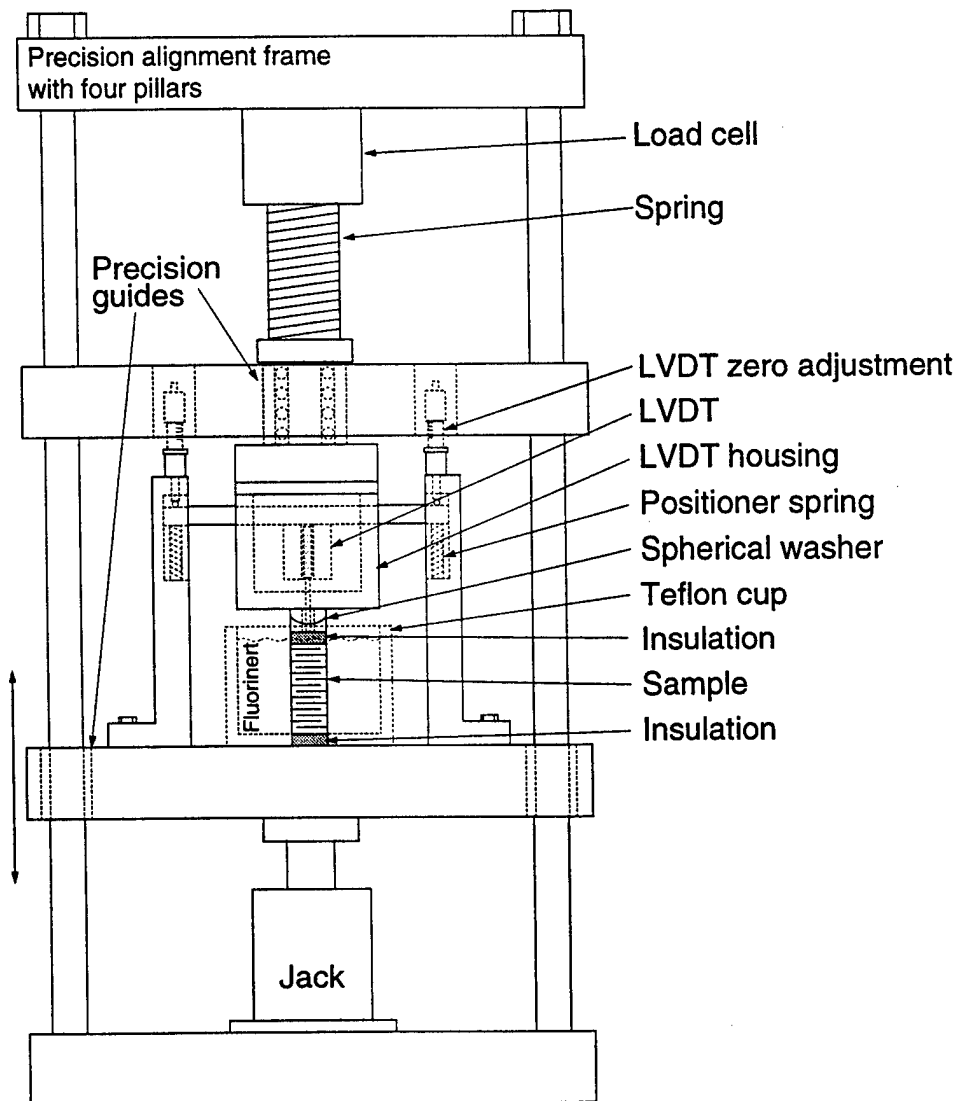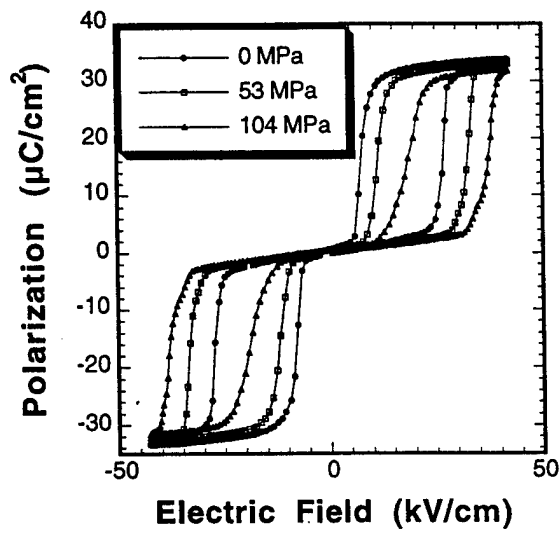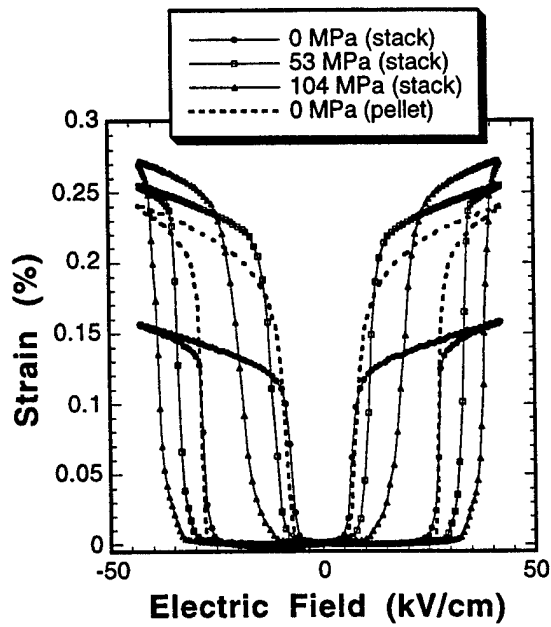
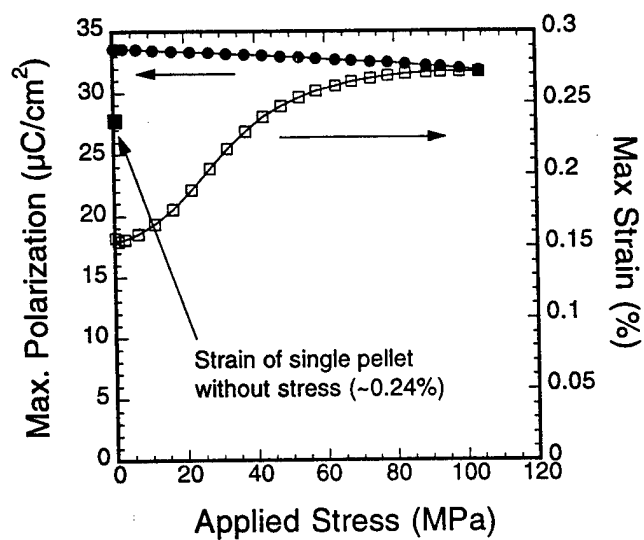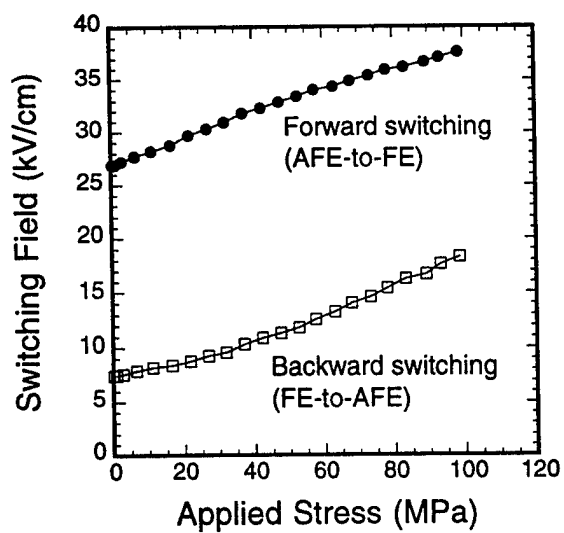Figure 1 The experimental setup for pre-stress measurements

(a)

(b)

Figure 2 (a) Polarization and (b) strain behaviors under various pre-stresses.

(a)

(b)

Figure 3 (a) Maximum polarization and strain and (b) switching fields as a function of pre-stress
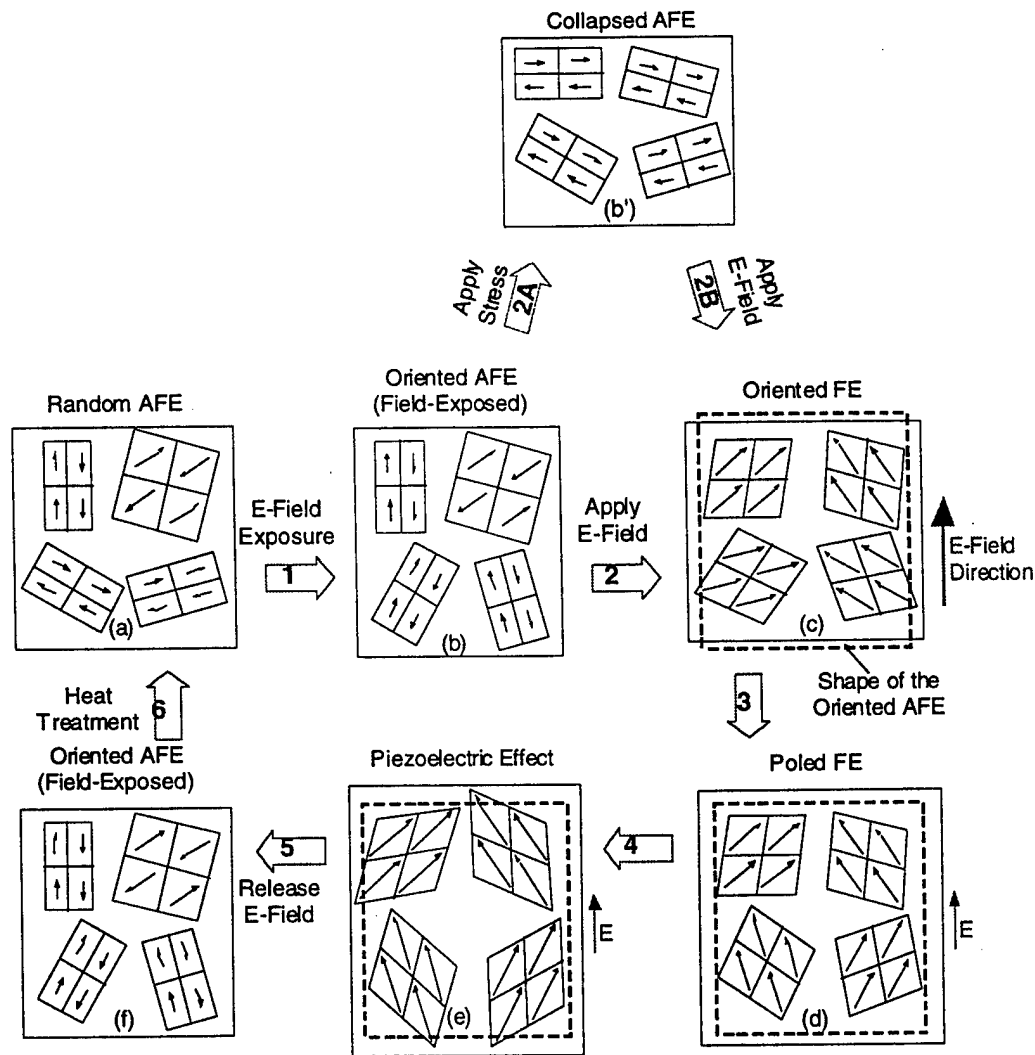
Figure 4 A schematic of the AFE-FE phase switching steps. The proposed extra steps 2A and 2B are caused by the uniaxial stress.

Table I The strain and hysteresis at various stresses and temperatures

	Strain (%)		Hysteresis (kV/cm)	
	0 MPa	60 MPa	0 MPa	60 MPa
21°C	0.144	0.252	21.3	21.0
50°C	0.137	0.230	14.3	15.0
75°C	0.124	0.191	9.1	9.5

Electroactive Actuator Materials:
Investigations on Stress and Temperature Characteristics

Ming-Jen Pan,[†] Patrick Pertsch,[*] Shoko Yoshikawa,
Thomas R. Shrout, and Venkata Vedula

Materials Research Laboratory
The Pennsylvania State University
University Park, PA 16802

ABSTRACT

The quasistatic electromechanical and dielectric behaviors of different electroactive actuator materials are investigated under the simultaneous influence of uniaxial stress and temperature at high driving field. An experimental setup capable of applying 9000 newtons of uniaxial force was carefully designed, based on a precisely guided steel frame. Extra caution was taken to minimize the effects of mis-alignment and contact surface clamping. The materials examined in this study include a prospective PLSnZT antiferroelectric ceramics which is currently under development, as well as electrostrictive ceramics, namely PMN-PT 90/10 and PMN-PT 76/24. To assess the applicability of these materials in real systems, multilayer stacks were assembled and their response to stress and temperature was examined. The overall strain of the PLSnZT composition showed increases with increasing uniaxial stress. This might be the result of re-orientation of antiferroelectric domains under pre-stress. It also showed excellent stability in strain over the temperature range 20 to 75°C under stress as high as 100 MPa. In contrast, the electrostrictive ceramics are less dependent on stress than antiferroelectrics but more susceptible to temperature changes.

Keywords: actuators, phase switching ceramics, antiferroelectrics, electrostrictive ceramics, lead magnesium niobate, pre-stress, temperature effect

1. INTRODUCTION

Ceramic actuators offer many characteristics that are attractive to smart structures applications, such as large generative force, fast response, low power consumption, and high volume efficiency. They are often used under large mechanical load or placed in pre-stressed conditions to maintain their integrity during service. In addition, actuators are often used in encapsulated environment where heat dissipation might cause local temperature increase. As a result, there has been a lot of interest in studying actuator response under pre-stress and temperature. Previous studies mostly have focused on the piezoelectric properties of various ferroelectrics.[1-4] In this study, we investigated two types of non-piezoelectric ceramics, namely electrostrictive and phase switching ceramics. Unlike piezoelectric materials which only involve ferroelectric domain reorientation, antiferroelectric materials also undergo a phase transition and change in unit cell dimensions. In contrast, lead magnesium niobate-lead titanate (PMN-PT) relaxors do not have ferroelectric domains before the application of an electric field.

Electrostrictive PMN-PT ceramics belong to a class of relaxor ferroelectrics which exhibit no macroscopic polarization. Upon the application of an electric field, dimensional change which is proportional to the square of the field-induced polarization can be observed. Because of the little hysteresis it exhibits and consequently little heat generation and excellent position repeatability, PMN-PT is attractive for precision submicron control. The most common composition is 90% PMN-10% PT (90-10) for room temperature applications. Also, a composition with higher PT content (76-24) and thus higher field-induced ferroelectricity has been identified for use at 85°C.[5] The dielectric constant versus temperature data for these two materials are plotted in Figure 1.

[†] Corresponding author: email: mjpan@psu.edu; Phone: (814) 863-2639; Fax: (814) 865-2326
[*] Visiting scientist from Fraunhofer-Institute for Applied Optics and Precision Engineering, D-07745 Jena, Germany.
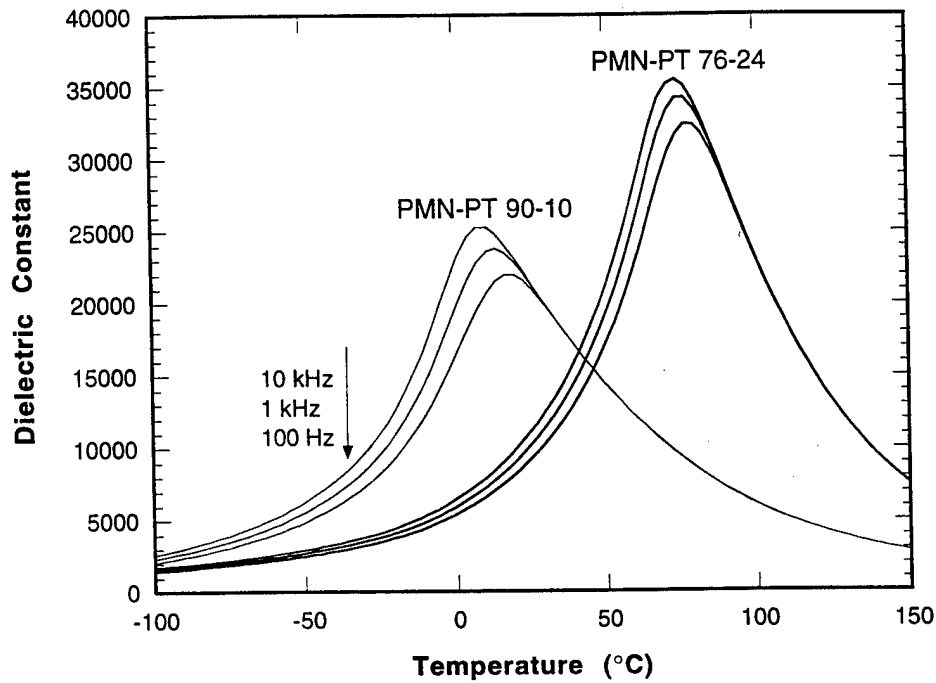
Figure 1 Temperature dependence of dielectric constant for PMN-PT 90-10 and 76-24.

The lead lanthanum stannate zirconate titanate (PLSnZT) system (Figure 2) has been widely studied for actuator applications due to its potential of producing high strain. In this family of ceramics, the antiferroelectric tetragonal (AFE_{tct}) phase can be readily switched to its neighboring ferroelectric rhombohedral (FE_{rh}) phase with the application of an electric field. This phase transition is accompanied by a large change in volume associated with high longitudinal strain (in the field direction). Crystallographic analyses based on X-ray diffraction have shown that 0.5% is the maximum strain possible for an ideal single
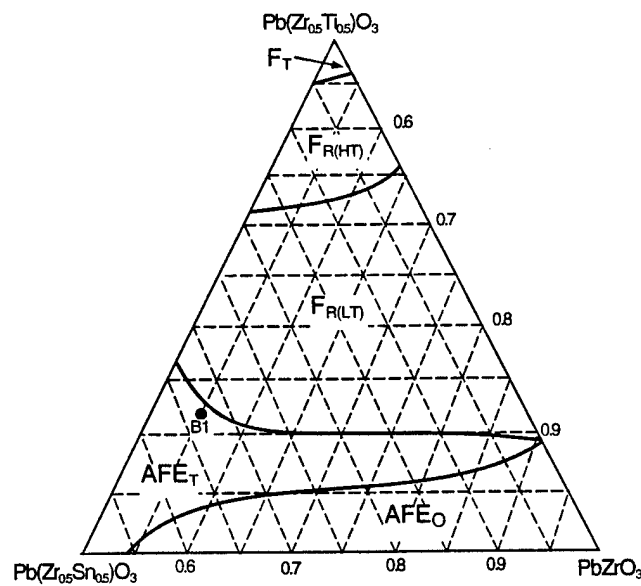

Figure 2 PLSnZT ternary phase diagram

crystal in this system.[6,7] For polycrystalline samples, a strain of 0.2% can be readily achievable at the antiferroelectric-to-ferroelectric (AFE-FE) switching field.[8] This study investigates the influence of pre-stress and temperature on the AFE-FE phase switching. A composition in the AFE_{tet} region, $(Pb_{0.98}La_{0.02})(Sn_{0.33}Zr_{0.55}Ti_{0.12})_{0.995}O_3$, was chosen for this study.

2. EXPERIMENTAL SETUP AND SAMPLE PREPARATION

An experimental setup was designed to measure the material and actuator response under both uniaxial stress and temperature (Figure 3). A rigid, precisely guided steel frame provides true uniaxial stress during loading. The spherical washer on top of the upper contact plate further minimizes transverse force and bending moment caused by non-parallel sample surfaces. A soft spring is used in the load train (3000 N maximum force with 160 N/mm stiffness or 9000 N with 480 N/mm stiffness) to provide relative constant load when the sample expands under an electric field. Due to the spring and some heavy mechanical parts, only quasi-static measurements can be performed on this setup (< 1 Hz).

During measurements, a desired pre-stress is first applied to the sample and then an electric field is applied. The field-induced polarization is measured using a Sawyer-Tower circuit. The displacement of the sample is monitored by a linear variable differential transformer (LVDT), which is driven by a lock-in amplifier. By using a lock-in amplifier, the LVDT resolution is in the range of 10 nanometers. Note that the LVDT assembly is not part of the load train, but part of the steel frame. The LVDT is attached to a pair of micrometer-controlled positioning fixtures, which are fastened onto the steel frame. So when a sample strains under an electric field, the LVDT senses the relative motion between the frame and the top of the sample. During measurement, the sample is immersed in an insulating liquid, Fluorinert™ (3M, St. Paul, MN, USA), to prevent arcing. A heating ribbon assembly, which can be inserted into the liquid-filled Teflon™ cup, allows the sample temperature to reach as high as 165°C (Figure 4).
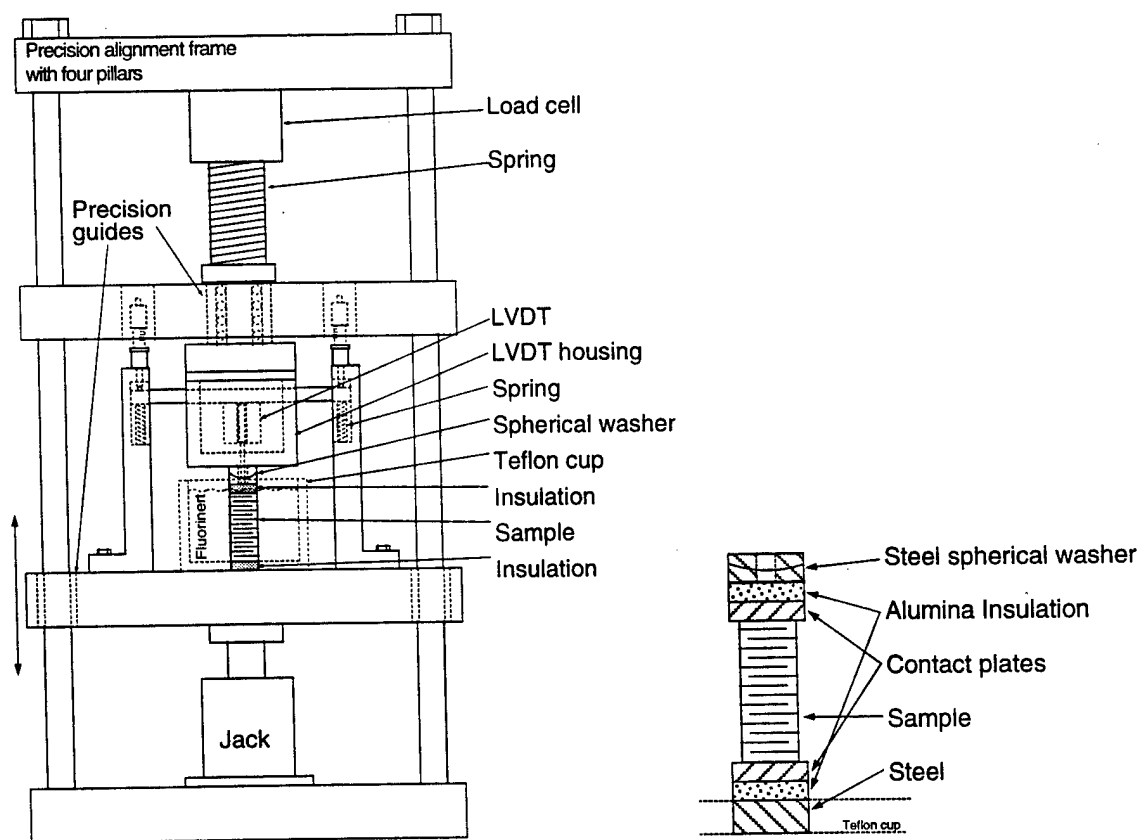

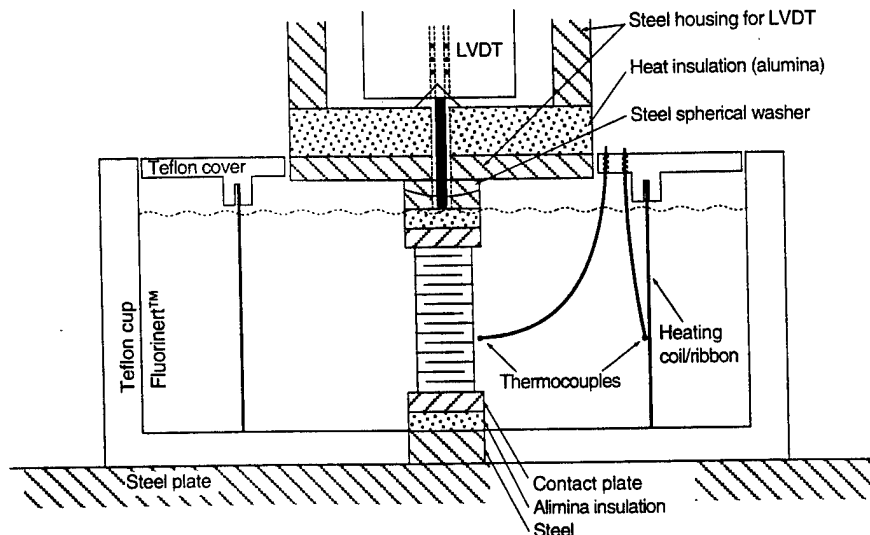Figure 3 A schematic of the experimental setup for pre-stress measurements

Figure 4 A schematic of the Teflon™ heating bath

A major concern in this type of measurement is the friction at sample/fixture surfaces. Therefore, efforts were made to reduce the effects of frictional clamping. The contacts plates have a mirror finish with an average surface roughness of $R_a = 5$ nm. The clamping effect can be further reduced by using samples with high aspect ratio. In this study multilayer stacks with 10.0 mm diameter and 10.7 mm in height are built for the measurements. Each stack has 16 active layers which have a thickness of 0.5 mm. Two passive endcaps at the top and bottom of the stack are made of the same material and were polished to $R_a = 75$ nm on the outer surfaces. The electrical contact of the discs is realized by 50 μm thick metal shims between the active layers.

3. ELECTROSTRICTIVE CERAMICS

Uniaxial stress up to 100 MPa was applied to various samples. During the measurements, pre-stressed samples expand under the applied electric field and the corresponding polarization and displacement were measured simultaneously. Shown in Figures 5(a) and 5(b) is the stress dependence of PMN-PT 90-10. Only small changes in polarization and strain were observed. At 100 MPa, the material still retains 85% and 68% of its stress-free polarization and strain, respectively. The hysteresis remained virtually unchanged for all stresses. Moreover, the strain versus polarization curves showed perfect parabolic shapes for all stresses (Figure 5c), indicating that the electrostrictive coefficient, Q_{111}, was independent of the applied stress. By using least square regression, the above coefficient was determined to be 0.0178 m^4/C^2.

PMN-PT 76-24 material, which has a higher dielectric maximum temperature due to its higher PT content, was tested at its operating temperature, 85°C. As shown in Figures 5(d) to 5(f), it had the same characteristics as PMN-PT 90-10, although its strain level was almost 50% higher than that of 90-10. This was not surprising because 76-24 is simply the high temperature version of 90-10. The electrostrictive coefficient Q_{111}, which was determined to be 0.0210 m^4/C^2, was also independent of stress.

Both materials were also subjected to various combinations of temperature and stress. For each condition, a unipolar (half sine wave) electric field with a 20 kV/cm maximum was applied to the sample. The results for PMN-PT 90-10 are plotted in figures 6(a) and 6(b). This shows that the field-induced polarization and strain decreased monotonically with increasing temperature as it moves away from its dielectric maximum and into the paraelectric region. The stress dependence of 90-10 remained similar for all temperatures. PMN-PT 76-24 displays the same behavior at temperatures higher than 85°C. At room temperature, however, a stress dependence typical of a normal "soft" ferroelectric material was seen. The observed
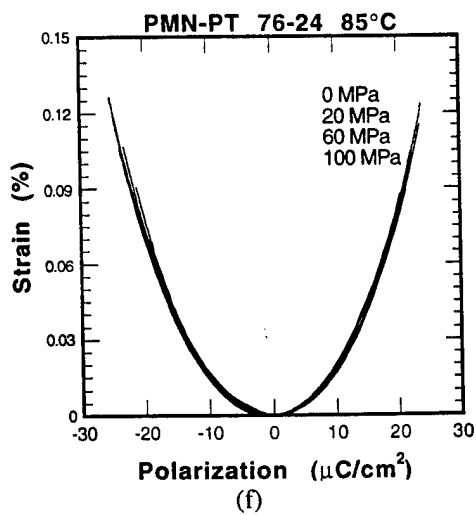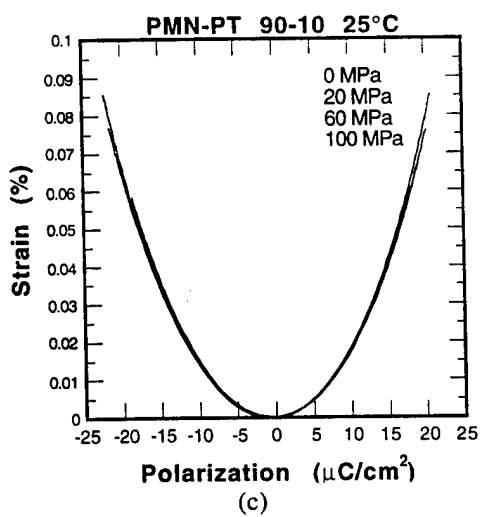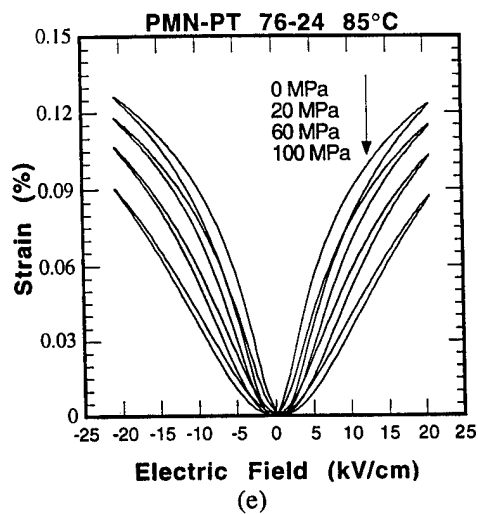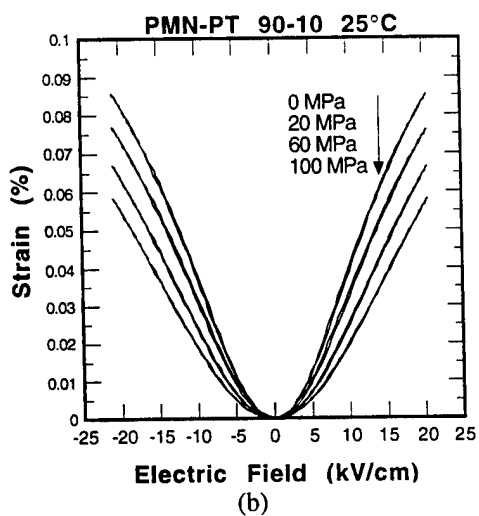
PMN-PT 90-10 25°C

(a)

PMN-PT 76-24 85°C

(d)

PMN-PT 90-10 25°C

(b)

PMN-PT 76-24 85°C

(e)

PMN-PT 90-10 25°C

(c)

PMN-PT 76-24 85°C

(f)
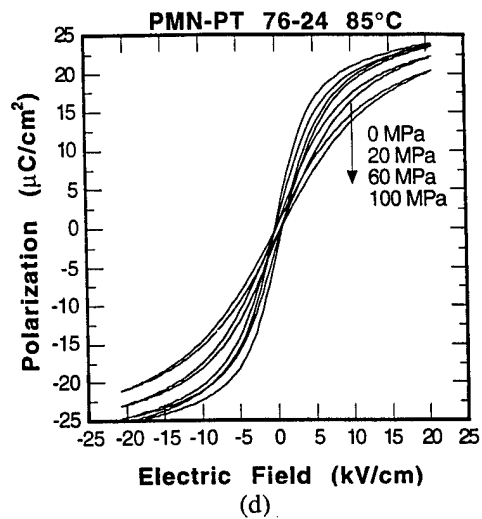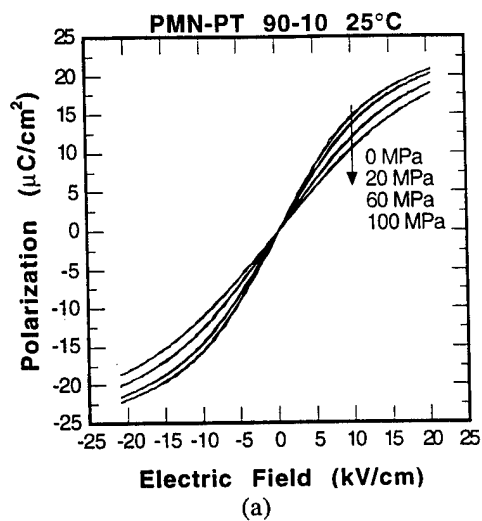
Figure 5   The polarization and strain behaviors of PMN-PT 90-10 ((a)-(c)) and 76-24 ((d)-(e))

PMN-PT 90-10

Polarization ($\mu C/cm^2$) vs Applied Stress (MPa)

25°C
45°C
60°C
85°C

(a)

PMN-PT 76-24

Polarization ($\mu C/cm^2$) vs Applied Stress (MPa)

85°C
105°C
125°C
25°C

(c)

PMN-PT 90-10

Strain (%) vs Applied Stress (MPa)

25°C
45°C
60°C
85°C

(b)

PMN-PT 76-24

Strain (%) vs Applied Stress (MPa)
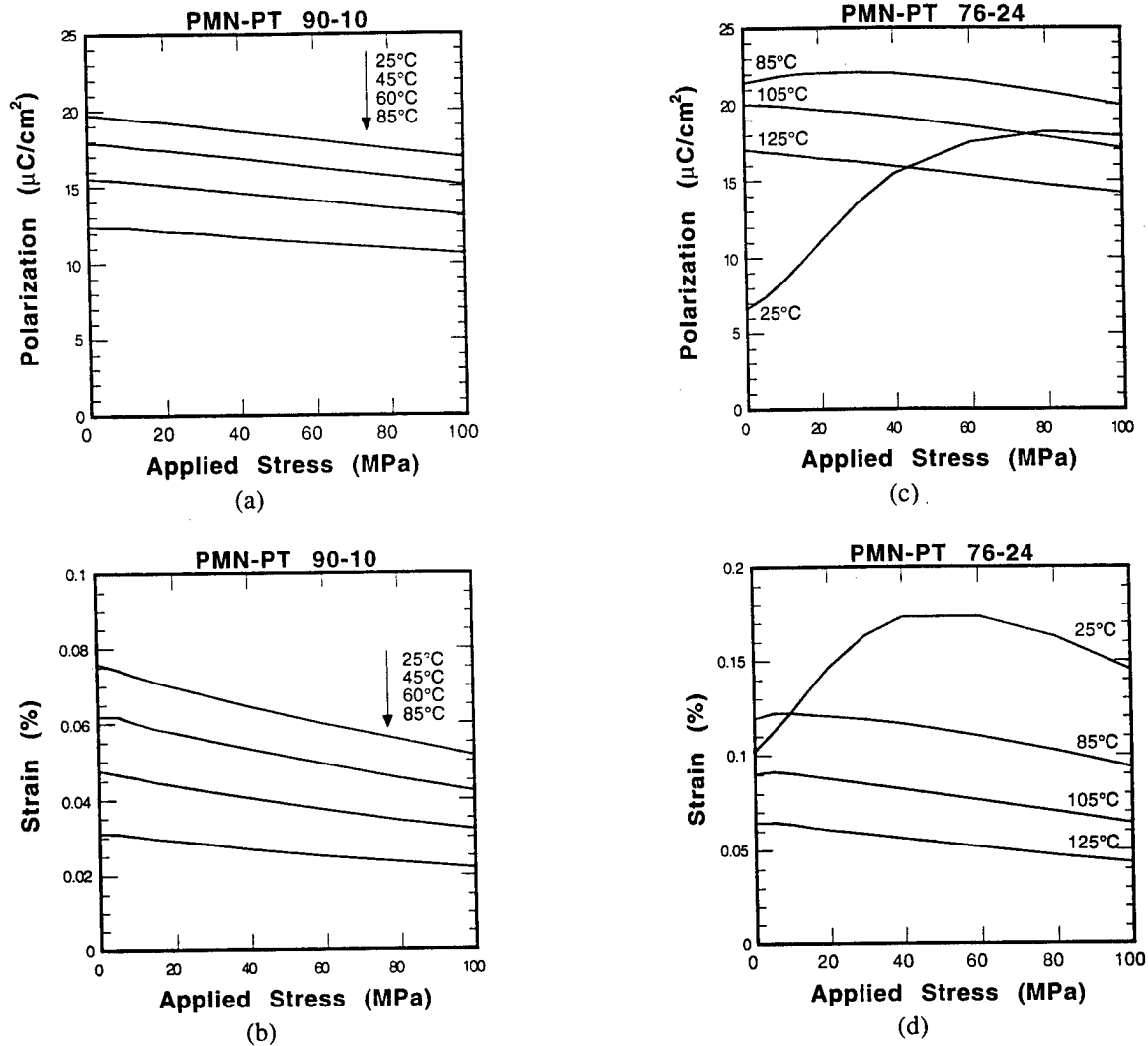
25°C
85°C
105°C
125°C

(d)

Figure 6   The polarization and strain of PMN-PT 90-10 and 76-24 under various combination of temperature and stress

behavior was the result of two competing processes: domain flipping due to stress (polar direction perpendicular to stress) and electric field (polar direction align with field). Similar behavior of soft piezoelectrics has been reported in the past.

4. PHASE SWITCHING CERAMICS

Like the electrostrictive materials, uniaxial stress up to 100 MPa was applied to the phase switching material. Some of the results are shown in Figure 7. It is interesting to observe that the overall strain increases with increasing pre-stress. As shown in Figure 8a, the strain at stresses greater than 80 MPa can be twice as high as that without pre-stress. At the same time, however, the polarization remained relatively unchanged, indicating that the AFE-to-FE phase switching was complete. Apparently, there was a decoupling between the polarization and strain. The pre-stress also increased the switching fields as shown in Figure 8b. Both the forward and backward switching fields have equivalent slopes of 0.11 kV/cm per MPa. The hysteresis (the difference between the forward and backward switching fields) remained constant at about 20 kV/cm.

To explain the above observations of phase switching behavior under uniaxial stress, we propose an addition to the switching sequence in Reference 9, as illustrated in Figure 9. It is possible that the AFE domains of a typical electric field-exposed sample (b) collapse under applied stress (b'). This makes the sample smaller in the stress direction. As a result, the
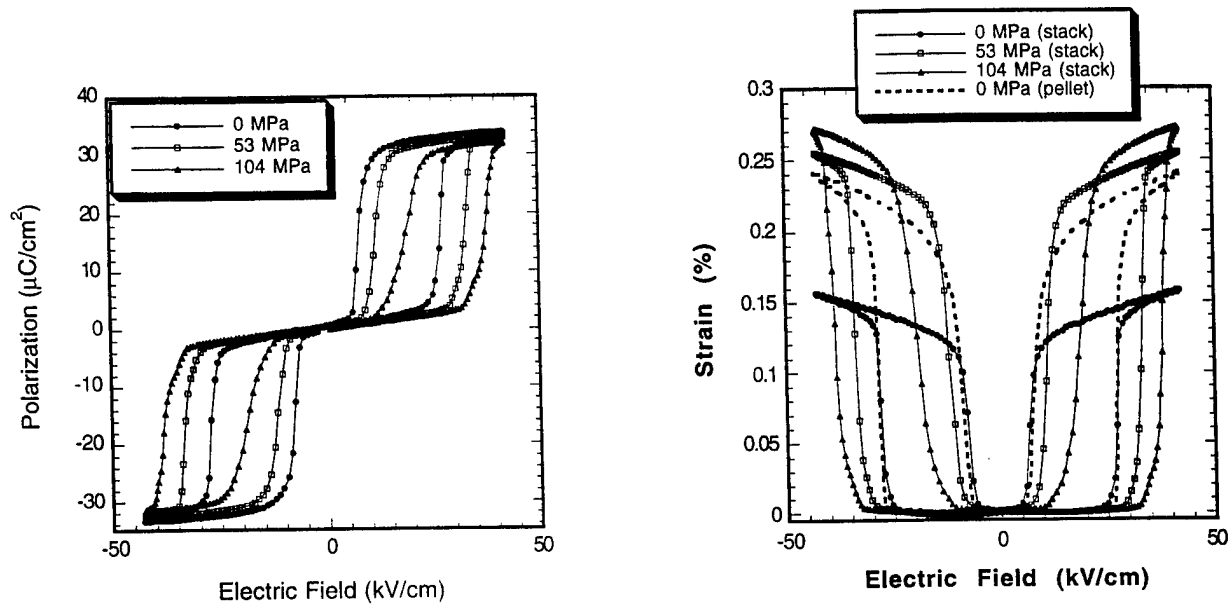
Figure 7 (a) Polarization and (b) strain behaviors under various pre-stresses

dimensional change in E-field direction between the AFE and FE states (b' to e) of a stressed sample is larger than that of a stress-free sample (b to e). The collapsed AFE domain state also implies that additional energy is needed during phase transformation when a sample stretches against the applied stress, which explains why the increased switching field under stress. Experimental confirmation of the proposed explanation, however, is still needed.

Finally, it was noted that the strain of multilayer samples, even without external stress, is more than 30% smaller than that of a single pellet (Fig. 8a). This reduction in performance was likely due to the multilayer structure. Specifically, the passive endcaps, shims and epoxy used for assembling the multilayer stacks constrain the active ceramic layers expansion in the transverse directions and caused a reduction of the longitudinal strain.
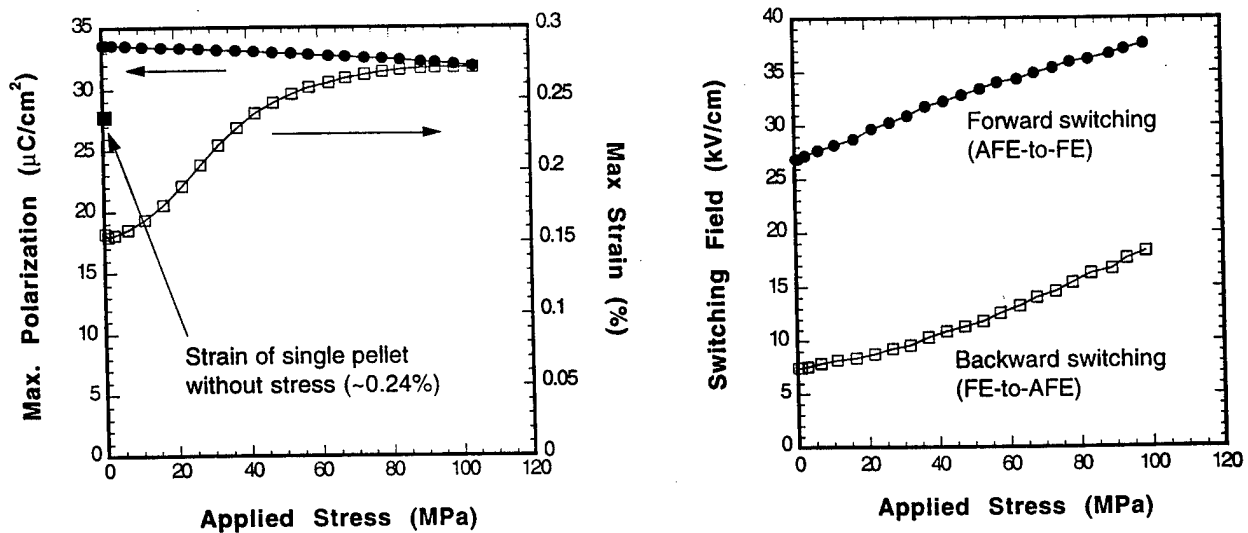

Figure 8 (a) Maximum polarization and strain and (b) switching fields as a function of pre-stress
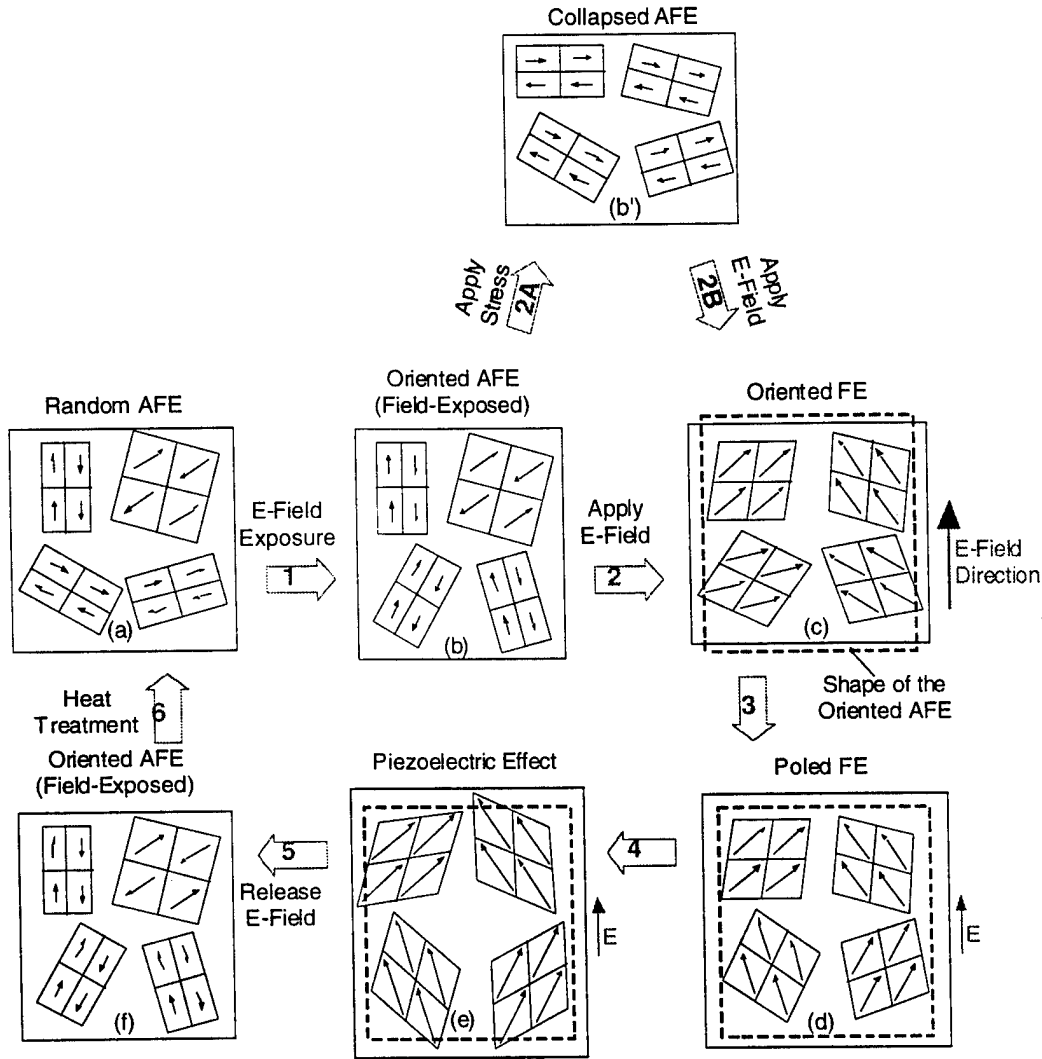
Figure 9   A schematic of the AFE-FE phase switching steps.   The proposed extra steps 2A
and 2B are caused by the uniaxial stress.

The effects of temperature on phase switching were also examined.   Because the epoxy used for assembling the
antiferroelectric multilayer stacks does not have high temperature capability, the measurements were performed only at 50 and
75 °C.   Table I is the summary of the strain and hysteresis under various stresses and temperatures.   The strain showed a
remarkable stability for the temperature range 20 to 75°C.   At 60 MPa, the strain at 75°C retained more than 75% of the
strain at 21°C.   This composition also displayed reduced hysteresis at higher temperatures.

5. SUMMARY

An experimental setup that applies up to 9000 N of uniaxial force was designed and built.   Extra caution was taken to prevent
any transverse movement or bending on samples.   The clamping effect at contact surfaces was minimized by using mirror
finish contact plates and high aspect ratio samples, i.e., multilayer stacks.   Two types of electroactive ceramics were
investigated in this study: electrostrictive and antiferroelectric materials.

Table I The strain and hysteresis at various stresses and temperatures of the antiferroelectric material in this study

	Strain (%)		Hysteresis (kV/cm)	
	0 MPa	60 MPa	0 MPa	60 MPa
21°C	0.144	0.252	21.3	21.0
50°C	0.137	0.230	14.3	15.0
75°C	0.124	0.191	9.1	9.5

For electrostrictive ceramics, PMN-PT 90-10 and its high temperature (85°C) counterpart 76-24, were tested. It was shown that neither electrostrictive PMN-PT is sensitive to external stress, while 76-24 showed superior electromechanical properties to 90-10. The electrostrictive coefficients for both materials were independent of stress. PMN-PT, nevertheless, was very sensitive to temperature change, because it was mostly operated at temperatures near its dielectric maximum. For the antiferroelectric material in this study, the strain at high pre-stress (>80 MPa) was almost twice as high as the strain without pre-stress. This is likely due to the AFE domain re-orientation process under load. The material also showed excellent stability in performance for the temperature range 20 to 75°C under various pre-stresses.

6. ACKNOWLEDGMENTS

7. REFERENCES

1. H.H. Krueger, "Stress Sensitivity of Piezoelectric Ceramics: Part 1. Sensitivity to Compressive Stress Parallel to the Polar Axis," *J. Acoust. Soc. Am.*, **42** [3] 636-645 (1967).
2. S.W. Meeks and R.W. Timme, "Effects of One-Dimensional Stress on Piezoelectric Ceramics," *J. Appl. Phys.*, **46** [10] 4334-38 (1975).
3. T. Inoue and S. Takahashi, "Measurements for Piezoelectric Ceramic Properties Applied Compressive Stress Parallel to the Polar Axis," *Trans. IECE Japan*, vol. E69, 1180-1187 (1986).
4. M. Kondo, K. Ohya, and S. Shimizu, "Effects of One-Dimensional Compressive Stress on the Properties of Multilayer Piezoelectric Ceramic Actuator," IEEE ISAF'90 pp.530-534.
5. W.S. Hackenberger, TRS Ceramics, Inc., private communication, 1997.
6. C.T. Blue, J.C. Hicks, S.-E. Park, S. Yoshikawa, and L.E. Cross, "*In situ* X-Ray Diffraction Study of the Antiferroelectric-ferroelectric Phase Transition in PLSnZT," *Appl. Phys. Lett.*, **68** [21] 2942-44 (1996).
7. L. Shebanov, M. Kusnetsov, and A. Sternberg, "Electric Field-Induced Antiferroelectric-to-Ferroelectric Phase Transition in Lead Zirconate Titanate Stannate Ceramics Modified with Lanthanum," *J. Appl. Phys.*, **76** [7] 4301-4 (1994).
8. K.A. Markowski, S.-E. Park, S. Yoshikawa, and L.E. Cross, "Effect of Compositional Variations in Lead Lanthanum Zirconate Stannate Titanate System on Electrical Properties," *J. Am. Ceram. Soc.*, **79** [12] 3297-304 (1996).
9. S.-E. Park, M.-J. Pan, K. Markowski, S. Yoshikawa, and L.E. Cross, "Electric Field Induced Phase Transition of Antiferroelectric Lead Lanthanum Zirconate Titanate Stannate Ceramics," *J. Appl. Phys.*, **82** [4] 1798 (1997).